Miscellaneous Publication 152

COMPARING CRITICAL SUPERSATURATIONS: ATMOSPHERIC CLOUD CONDENSATION NUCLEI VS. KNOWN COMPOUNDS

BY

WILLIAM BARRETT EVANS

B.S., University of Illinois at Urbana-Champaign, 1991

THESIS

Submitted in partial fulfillment of the requirements
for the degree of Master of Science in
Environmental Engineering in Civil Engineering
in the Graduate College of the
University of Illinois at Urbana-Champaign, 1994

Urbana, Illinois

Illinois State Water Survey
Atmospheric Sciences Division
A Division of the Illinois Department of Energy and Natural Resources

COMPARING CRITICAL SUPERSATURATIONS: ATMOSPHERIC CLOUD CONDENSATION NUCLEI VS. KNOWN COMPOUNDS

BY

WILLIAM BARRETT EVANS

B.S., University of Illinois at Urbana-Champaign, 1991

THESIS

Submitted in partial fulfillment of the requirements
for the degree of Master of Science in
Environmental Engineering in Civil Engineering
in the Graduate College of the
University of Illinois at Urbana-Champaign, 1994

Urbana, Illinois

ABSTRACT

Cloud Condensation Nuclei (CCN) are microscopic particles in the atmosphere which develop into water droplets when exposed to supersaturated conditions. The clouds formed by these droplets have a significant effect on the global climate. The purpose of this research was to experimentally determine the behavior and chemical composition of actual CCN particles. This was achieved by using captured CCN from a system including a cloud chamber and several virtual impactors. The captured CCN material was then resuspended as dry particles. This aerosol was then passed through a classifier and a cloud chamber in order to determine the critical radius and corresponding critical supersaturations of the CCN material. These data were then compared to similar data taken for suspected CCN materials. This comparison indicated that the activation characteristics of total CCN and large CCN ($0.1 < d_p < 0.5$ μm) are controlled by the ammonium sulfate present in the particles. This was verified both graphically and numerically. The numerical method involved developing Ω, the number of ions per unit volume formed by dissolution of the CCN material. Ω was also calculated for organic compounds of unknown composition which were discovered in the actual CCN samples by chemical analysis. This value was $\Omega_{organics} = 26{,}425.3$. This is smaller than the Ω. for ammonium sulfate (40,095.5), indicating that the organic material is less active than ammonium sulfate. Thus, the presence of the organics acts to slightly retard droplet formation on large CCN. The organic compounds are not, however, so inactive that they could not nucleate under naturally occurring supersaturated conditions. Using $\Omega_{organics,}$ it was calculated that particles as small as 0.03 (μ m in diameter which consisted entirely of the organic compounds could activate under natural conditions. This size is well within the observed size range for actual CCN.

ACKNOWLEDGMENTS

There are many people who deserve mentioning for their support of this research. First of all, I would like to thank my advisor, Dr. Allen Williams of the Illinois State Water Survey, for funding as well as guiding my work. Without him, none of this would have been possible. I would also like to thank my academic advisor, Professor Susan Larson, for her continual support. Finally, a hearty thank you to Kent McClure, Tim Mahannah, Jim Osborne, and Paul Nelson. Without their technical expertise, constructing the experimental setup would have been almost impossible.

TABLE OF CONTENTS

LIST OF TABLES

LIST OF FIGURES

LIST OF SYMBOLS

a = curvature term
A = curvature term (Alofs' notation)
b_N = solute term
B = solute term (Alofs' notation)
B_c = B value at maximum S_r
B_0 = B value at very large X_e
d = plate spacing for a CFD chamber
d* = Kelvin diameter for a droplet
d_p = diameter of a particle
D = diffusion coefficient of water vapor
dr/dt = growth rate of a droplet
h = distance of hot plate from cold plate in a CFD chamber
i = van't Hoff factor
L = latent heat of condensation
m = mass
m_N = effective nucleus mass
M = molecular weight
M_N = molecular weight of nucleus material
M_s = molecular weight of dissolved salt
M_w = molecular weight of water
M_0 = molecular weight of water (Fletcher's notation)
p = actual partial pressure of vapor
p_s = saturation vapor pressure for a flat liquid surface
r = radius
r_c = critical radius
R = ideal gas constant
S = supersaturation
S_{aVg} = average supersaturation
S_c = critical supersaturation
S_{max} = maximum supersaturation
S_r = saturation ratio
T = absolute temperature
T_c = cold plate temperature for a CFD chamber
T_h = hot plate temperature for a CFD chamber
V_c = minimum centerline velocity for a CFD chamber
X_O = equilibrium size of a droplet
X_e = equilibrium diameter of a hygroscopic particle
X_0 = dry diameter of a particle
z = distance from cold plate in a CFD chamber
e = volume of soluble matter per total volume of dry particle
e_m = mass fraction of soluble material in a particle
e_v = volume fraction of soluble material in a particle
Θ = temperature
Θ_1 = temperature of cold plate of a CFD chamber in K
$\underline{\Theta_2}$ = temperature of hot plate of a CFD chamber in K
Θ = mean temperature of the two plates of a CFD chamber
K = thermal conductivity of air
p = density
p_L = density of liquid water

ρ_s = density of a solution
ρ_v = vapor density
ρ_w = density of water
ρ_o = density of particle in its dry state
σ = surface tension of a liquid
ϕ = osmotic coefficient of a solution
ϕ_c = ϕ value at maximum S_r
ϕ_0 = ϕ value at very large X_e
Ω = composition factor for CCN material
Ω_{amsul} = Ω value for ammonium sulfate
Ω_{CCN} = Ω value for CCN
$\Omega_{organics}$ = Ω value for organic compounds

Chapter 1

Introduction

1.1 Cloud Condensation Nuclei

Cloud Condensation Nuclei (CCN) are microscopic particles in the atmosphere which develop into water droplets when exposed to the supersaturated conditions present in clouds. Supersaturation is the measure of the excess of water vapor above 100% relative humidity (RH) (Twomey, 1977a). For example, 101% RH is equal to 1% supersaturation. The supersaturations which naturally occur in clouds are usually of the order of a few tenths of a percent, but can reach as high as 1% (Twomey, 1977a). Measurements have shown that most CCN range from 0.02 to 0.04 μm in diameter (Twomey and Severynse, 1964; Twomey, 1972; Twomey, 1977b; Fitzgerald et al., 1982). This small size puts CCN on the upper end of the nucleation mode. Their size also makes direct measurement of the chemical composition of CCN nearly impossible. The purpose of this research is to determine the activation (droplet formation) characteristics of CCN in known supersaturated conditions by comparing the behavior of the soluble portion of actual CCN to the behavior of compounds which are suspected to be major components of CCN.

1.2 The Importance of CCN

The CCN in the atmosphere produce the water droplets which make up clouds. These clouds can either absorb or reflect sunlight, thus altering the radiative balance of the earth. The absorption of sunlight by cirrus clouds warms the atmosphere while reflection by stratocumulus clouds cools it (Monastersky, 1989). On average, stratocumulus clouds cover 34% of the globe while cirrus clouds cover only 16% (Monastersky, 1989). Therefore, there is an overall global cooling effect from cloud cover. Global modeling performed by Wigley (1989) showed that an increase in CCN, which would result in increased cloud albedo, would increase this cooling effect. The recent fears of global warming due to increased anthropogenic CO_2 emissions brought about a large number of

studies on the ability of CCN to cool the planet. Early calculations by Twomey (1977c) linked possible global changes in planetary albedo to changes in CCN. Further research using numerical models indicated that a doubling of the atmospheric CO_2 concentration might theoretically be offset by the cooling effect of a doubling of the CCN concentration (Wigley, 1989; Twomey et al., 1984; Charlson et al., 1987). Whether or not a CCN concentration increase would coincide with an increase in CO_2 emissions depends upon the major sources of CCN. If the CCN are primarily anthropogenic, an increase concurrent with a CO_2 increase could be expected. If, however, the CCN come from a natural source, a simultaneous increase may not occur. Without an understanding of future CCN concentrations, it will be impossible to accurately predict the extent to which global warming will occur. An accurate understanding of the CCN sources is especially important since small aerosols like CCN have an atmospheric lifetime of a few days (Hinds, 1982), while CO_2 has a lifetime of around 15 years (Seinfeld, 1986). This large difference in residence times requires a good understanding of CCN sources and how they will change over time in order to project the ability of CCN to continue to offset the ever increasing CO_2 concentrations.

1.3 Previous Studies of CCN Chemical Composition

Previous attempts to determine the chemical composition and sources of CCN have had limited success. Problems arise due to the small size of CCN and their low concentrations, typically only a few hundred per cubic centimeter, in the atmosphere (Twomey, 1977a). Their small size does, however, give some indication of their composition. Measurements of actual CCN sizes indicate that the majority are 0.02 to 0.04 μm in diameter (Twomey and Severynse, 1964; Twomey, 1972; Twomey 1977b; Fitzgerald et al., 1982). Twomey (1977a) used nucleopore filters as a diffusion battery to remove selected sizes of atmospheric CCN before passing the remaining CCN particles through a cloud chamber. The air flowrate through the filter was reduced to increase the

removal (by diffusion to the filter pore walls) until droplets were no longer seen in the cloud chamber. Using the diffusion equation, Twomey (1977a) calculated that the mean radii of the CCN must be smaller than 0.03 μm (d_p < 0.06 μm). CCN activation at supersaturations less than 1% is also well documented (Twomey, 1977a). At these low supersaturations, nucleation theory for insoluble materials requires a dry particle radius of at least a few tenths of a micrometer (Twomey, 1977a). For example, at a supersaturation of 1%, the critical (minimum) dry particle radius for a droplet to form on a wettable insoluble particle is 0.12 μm (Twomey, 1977a). This is much larger than the observed sizes of the majority of CCN particles. Smaller particles consisting of soluble materials, however, can activate to form droplets at these supersaturations (Twomey, 1977a). This is due to the lowering of the equilibrium vapor pressure above the droplet surface which is brought about by the presence of a dissolved material such as a salt (Hinds, 1982). Therefore, it is evident that a majority of CCN must be composed at least partially of soluble rather than insoluble materials. This is not to say that wettable insoluble particles greater than a diameter of 0.12 μm do not exist, for they most likely do. These particles will activate to form droplets and thus affect the overall chemistry of CCN particles, especially the large CCN. The small CCN, however, will be dominated by particles which are at least partially soluble. Several theoretical studies have determined that atmospheric aerosols could consist of mixtures of soluble and insoluble substances (Junge and McLaren, 1971; Winkler, 1973; Hanel, 1976). These internally mixed particles could theoretically act like soluble particles if the soluble material was at the surface of the particle.

Another problem with attempting to directly measure the chemical composition of CCN is that they must first be separated from all non-CCN particles in the atmosphere. One way to do this is to activate the CCN using some type of cloud chamber. Once activated, however, the original CCN materials become greatly diluted. Some measurements have been made despite this problem. A large amount of indirect evidence

"points to sulfates as the main constituent of CCN" (Meszaros, 1968; Twomey, 1971; Junge, 1972; Charlson et al., 1974; Whitby, 1978; Georgi, 1978; Ono and Ohtani, 1980; Cobourn and Husar, 1982; quote from Williams et al., 1992). Preliminary studies of bulk aerosol (all atmospheric particles) found ammonium sulfate and sodium chloride to be the two major soluble inorganic salts in the atmosphere (Twomey, 1977a). A later study of marine aerosols by Bigg (1990) found that 80 to 90% of particles less than 0.2 μm in diameter consisted of ammonium sulfate while the rest were either sodium chloride or an unknown, insoluble liquid. Twomey (1977a) used the greater volatility of ammonium sulfate compared to sodium chloride in an attempt to determine which of the two (ammonium sulfate or sodium chloride) was the main constituent in CCN. He did so by first passing an aerosol composed of natural atmospheric CCN particles through a heated tube. The number of particles present downstream of the heater was counted at increasing temperatures until eventually all of the particles were volatilized. This same procedure was then repeated for laboratory aerosols of sodium chloride, ammonium sulfate, and several other ammonium salts. The results of this experiment showed the responses of the natural CCN particles and the ammonium sulfate to be almost identical, while the sodium chloride volatilized at a much higher temperature. Therefore, it appears that most of the atmospheric CCN particles are either "ammonium sulfate or some other substance with similar volatility" (Twomey, 1977a). Recent direct measurements of CCN chemistry have indicated sulfate as the main negative ion, and NH_4^+, Na^+, K^+ and H^+ as the positive ions (Harrison, 1985; Rosinski et al., 1984).

1.4 Sulfates and CCN

The large amount of preliminary evidence which points to sulfates as a major, if not the dominant, constituent in CCN calls for an examination of possible sulfate sources. Williams et al. (1992) suggested that perhaps abundant sulfur is always present in the atmosphere, and that the positive ions are the "rate-limiting constituents." This abundance

of sulfur in the atmosphere suggests a possible link between CCN concentrations and SO_2 emissions. These emissions could either be from anthropogenic sources or natural sources. The main anthropogenic source would most likely be the combustion of fossil fuels, especially coal. If this is true, then increasing SO_2 emissions could coincide with increasing CO_2 emissions and the global warming effects could be offset by the greater number of CCN present in the atmosphere (Wigley, 1989). The SO_2 emissions might be coming from a natural source such as phytoplankton in the oceans which release dimethylsulfide into the atmosphere (Charlson et al., 1987). If this case is true, then the number of CCN in the atmosphere would most likely not increase with increasing anthropogenic CO_2 emissions (Charlson et al., 1987). Therefore, it is important that the sources of CCN be determined as well as the chemical composition. This paper, however, shall only deal with the question of chemical composition.

1.5 Organics and CCN

To date, little work has been done to study the possibility of organics in CCN. Recent studies, however, seem to indicate that organics are indeed present in varying quantities in CCN. In order to study this possibility, Bigg (1986) used a diffusion cloud chamber with water to collect CCN. The collected CCN were then dried and reactivated in a chamber with first ethanol and then cyclohexane as the condensing vapors (instead of water). By using cyclohexane instead of water, it was possible to nucleate atmospheric CCN particles excluding those consisting solely of ammonium sulfate since ammonium sulfate particles do not appreciably activate in cyclohexane (Bigg, 1986). Bigg's study found that the majority of the CCN particles in the samples he collected contained an appreciable amount of a material (most likely hydrocarbons) which caused them to activate in cyclohexane vapors (Williams et al., 1992; Bigg, 1986). A comparison of measurements on land and at sea indicates that marine air contains much greater numbers of cyclohexane-CCN (Bigg, 1986). The larger amount of organics in marine air could be due

to organic films on the ocean surface which are broken by wave action, as postulated by Blanchard (1964). Preliminary examinations of CCN captured for this research also showed that a significant portion of the material is organic (Williams et al., 1992). Attempts to determine whether the organics are sampling artifacts due to the apparatus or actually part of the CCN indicate that the organics are indeed present in the atmospheric CCN particles.

There are several possible ways for organics to be present in atmospheric aerosols. One way is for the dry particle to consist either partially or entirely of organic materials. Such particles are called particulate organic matter (POM) (Williams et al., 1992). Ketseridis and Eichman (1978) found total POM concentrations of almost 10 $\mu g/m^3$ in samples taken off of the coast of Ireland. These samples contained nearly 500 organic compounds. This mass concentration is several orders of magnitude greater than the estimated CCN mass concentration in the atmosphere of 10-100 ng/m^3 (Williams et al., 1992). Another form in which organics can be part of atmospheric particles is as surface active films or surfactants (Rood et al., 1991; Williams et al., 1992). A considerable amount of research has been performed in an attempt to determine the effects of surfactants on droplet growth. Aerosol samples taken in California by Husar and Shu (1975) showed evidence of the presence of surfactant films. Later research by Gill and Graedel (1983) identified more than 80 organic surfactants which commonly occur in the atmosphere. It should be noted, though, that surfactants are usually thought to be agents which retard the growth of droplets (Rood et al., 1991). But with such a large number of organic surfactants present in the atmosphere, it would not be unrealistic for one or more to play an active role in CCN. Work by Andrews and Larson (1993) found that certain organic surfactants can enable normally hydrophobic particles, such as carbon black particles, to "sorb significant amounts of water." Thus, the presence of such surfactants could act to increase the number of potential CCN particles in the atmosphere.

1.6 Theory: Supersaturation vs. Dry Particle Radius

Several paths exist for the formation of water droplets in the atmosphere. These include homogeneous nucleation, heterogeneous nucleation on an insoluble particle, and heterogeneous activation of a soluble particle (Hinds, 1982). Homogeneous nucleation is the formation of water droplets from a supersaturated vapor without condensation nuclei (Hinds, 1982). This process rarely occurs in the atmosphere, so it will not be discussed in relation to this research. Heterogeneous nucleation on an insoluble particle does occur naturally in the atmosphere. However, since CCN are believed to mainly consist of soluble materials, this process will not be discussed in detail. Heterogeneous activation of soluble particles will be examined in detail, however. For detailed explanations of all of the methods of droplet formation, refer to either Hinds (1982) or Twomey (1977a).

Heterogeneous activation is the formation of water droplets by the condensation of water vapor onto a dry nucleus (particle) (Hinds, 1982). Since the particles which serve as nuclei have sharply curved surfaces, a greater partial pressure is required to prevent evaporation from the particle surface than for a flat surface (Hind, 1982). This is called the Kelvin Effect. It is possible to relate the saturation ratio (p/p_s) required for equilibrium above a droplet and the droplet size for a pure liquid (usually water) using the Kelvin or Thomson-Gibbs equation (Hinds, 1982),

$$S_r = \frac{p}{p_s} = \exp\left[\frac{4\sigma M}{\rho R T d^*}\right] \qquad (1.1)$$

where,

S_r = saturation ratio
p_s = saturation vapor pressure for a flat liquid surface
p = the actual partial pressure of vapor
σ = surface tension of the liquid
M = molecular weight of the liquid
ρ = density of the liquid
d^* = the Kelvin (equilibrium) diameter for the droplet
R = ideal gas constant
T = absolute temperature

This equation is for insoluble particles, but is also important in developing a relation for soluble nuclei since soluble particles also experience the Kelvin effect. When dealing with soluble nuclei, a new term must be added to the equation. According to Raoult's Law, the presence of a dissolved salt in water lowers the equilibrium vapor pressure above the water surface (Hinds, 1982). This is often referred to as the Solute Effect. The Solute Effect allows for activation to occur at a lower supersaturation with a soluble nuclei than with an insoluble one (Hinds, 1982). Thus, for soluble particles, there are two competing effects which control the relationship between the saturation ratio and the particle size required for growth (Hinds, 1982). As a droplet evaporates, the Kelvin Effect increases the vapor pressure due to the increase in the surface curvature of the droplet. At the same time, however, the concentration of salt in the droplet is increasing since only the water is evaporates, leaving a constant amount of salt (Hinds, 1982). This decreases the vapor pressure above the droplet by the Solute Effect. These two effects are combined in the following equation for soluble nuclei which was developed by combining Equation (1.1) and Raoult's Law (Hinds, 1982):

$$S_r = \frac{p}{p_s} = \left(1 + \frac{6imM_w}{M_s \rho \pi d_p^3}\right)^{-1} \exp\left[\frac{4\sigma M_w}{\rho R T d_p}\right] \qquad (1.2)$$

where,

m = mass of the dissolved salt
M_s = molecular weight of the dissolved salt
M_w = molecular weight of the solvent (water)
i = van't Hoff factor = # of ions each molecule of salt forms
d_p = diameter of the particle
p = density of the solvent (water)

Equation (1.2) was expanded and the leading terms yielded Equation (1.3) (Twomey, 1977a).

$$S = \frac{a}{r} - \frac{b_N}{r^3} \qquad (1.3)$$

where,

$$a = \frac{2\sigma M_W}{\rho_s R T} \qquad (1.4)$$

and,

$$b_N = \frac{i m_N}{(4\pi/3)\rho_s} \qquad (1.5)$$

where,

$$m_N = \text{effective nucleus mass} = (\text{mass of nucleus})\frac{M_W}{M_N}$$

and,

S = the supersaturation = S_r - 1
r = droplet radius
M_w = molecular weight of water
M_N = molecular weight of the nucleus material
i = van't Hoff factor
R = ideal gas constant
T = absolute temperature
σ = surface tension of the solution ≈ surface tension of water
p_s = density of solution ≈ density of water

A plot of either of these two relations (Equation (1.2) or (1.3)) for a given particle provides what is called a Kohler curve. A Kohler curve is a plot of droplet diameter versus the supersaturation and is specific for a certain solution composition (Hinds, 1982). More detail on the development of Equations (1.2) and (1.3) as well as on Kohler curves is available in both Hinds (1982) and Twomey (1977a).

The maximum or "critical" supersaturation, S_c, attained by a given particle before activation can be found using a slightly different relation which is derived in Twomey (1977a) from Equation (1.3) by equating its slope to zero, giving:

$$S_c = \frac{2a}{3r_c} = \frac{2}{3\sqrt{3}} a^{3/2} b_N^{-1/2} \qquad (1.6)$$

where r_c is the "critical radius" of the particle and a and b_N are the same as shown in equations (1.4) and (1.5), respectively. Equation (1.6) is the one that will be used frequently in this research since the critical supersaturation (S_c) and the critical radius (r_c) of the CCN are of greatest interest.

The droplet growth theory has been expanded upon since its original development to allow for the examination of particles which are a combination of soluble and insoluble materials. Junge and McLaren (1971) were the first to consider the possibility of calculating cloud nuclei spectra for varying soluble material content. An important parameter in this consideration is e, which is the fraction of soluble matter as given by

$$\varepsilon = \frac{\text{volume of soluble matter}}{\text{total volume of dry particle}} \qquad (1.7)$$

where e can vary from 0 to 1 (e = 0 for completely insoluble). The preliminary results from that research indicate that a combined soluble/insoluble particle will activate as a 100% soluble particle as long as the soluble content of the particle was above 10% (Junge and McLaren, 1971). Hanel (1976) also developed an equation which was then rearranged by Fitzgerald et al. (1982) to obtain a relation between the equilibrium diameter of a hygroscopic particle and the saturation ratio of the air surrounding it. This equation was once again rearranged by Alofs et al. (1989). This final form is the one which shall be used for this research when considering mixed composition particles. The Alofs et al. (1989) equation is as follows:

$$S_r = \exp\left(\frac{2A}{X_e}\right)\exp\left(-\frac{B}{\left(X_e^3/X_0^3\right) - 1}\right) \qquad (1.8)$$

where,

$$A = \frac{\sigma}{\rho_w R T} \qquad (1.9)$$

and,

$$B = \frac{\rho_0 i\, \phi \varepsilon_m M_w}{\rho_w M_s} \qquad (1.10)$$

or,

$$B = \frac{\rho_s i\, \phi \varepsilon_v M_w}{\rho_w M_s} \qquad (1.11)$$

For these equations, the variables stand for the following (Alofs et al., 1989):

S_r = the saturation ratio = 1 + S_c
X_e = the equilibrium diameter of a hygroscopic particle
X_0 = the dry diameter of the particle
T = the absolute temperature
R = the specific gas constant of water vapor
M_w = the molecular weight of water
M_s = the mean molecular weight of the soluble material
a = the surface tension of the droplet
ρ_w = the density of water
ρ_0 = the density of the particle in its dry state
ρ_s = the density of the soluble material
i = van't Hoff factor = # ions formed/ molecule of solute
ϕ = osmotic coefficient of the solution (ϕ = 1 for dilute solutions)
ε_m = the mass fraction of soluble material in the particle
ε_v = the volume fraction of soluble material in the particle

The term B is the "particle composition parameter" for dry nuclei which relates the behavior of particles in humid or supersaturated conditions to the composition of the particle (Fitzgerald et al., 1982). Note that B corresponds to b_N of the Kohler Theory. Its value varies with X_e, mainly because of the osmotic coefficient. The values of the osmotic coefficient and of B as functions of S_r and X_e are discussed in Alofs et al. (1989). In summary: the osmotic coefficient is a function of the molality of the solution droplet. The value of B at the maximum S_r is called B_c. At very large values for X_e, B is called B^0. The corresponding values of the osmotic coefficient are ϕ_c and ϕ^0. Since the osmotic coefficient for very dilute solutions is unity, $\phi^0 = 1$. Fitzgerald et al. (1982) performed several experiments in an attempt to determine the value of B_c. Measurements for particles ranging from 0.03 to 0.08 μm in radius gave a range of B_c values from 0.10 to 0.40, with an average value of 0.23 (Fitzgerald et al., 1982). These values can be converted to ε_v values for easier comparison using the following relation from Alofs et al. (1989)

$$\varepsilon_v = 1.587 B_c \qquad (1.12)$$

Note that Equation (1.12) is only true for particles whose soluble fraction consist entirely of ammonium sulfate (Alofs et al., 1989). Using this relation gives values for ε_v ranging from 0.1587 to 0.6348 with an average value of 0.37 for the Fitzgerald et al. (1982) data.

It also appears from these data that B_c, and therefore ε_v, decrease with increasing particle size. Alofs et al. (1989) performed a slightly different experiment in an attempt to determine the ε_v (the volume fraction of soluble material) of actual atmospheric particles (using the assumption that the only soluble material present is ammonium sulfate). For particle sizes ranging from 0.2 to 0.4 (xm in diameter, they found a mean ε_v value of 0.5. Other measurements made by Fitzgerald and Hoppel (1984) gave a mean ε_v of 0.46. Sekigawa (1983) also reported a mean value for ε_v of 0.5 for a particle size range of 0.05 to 0.2 μm in diameter. Thus, it appears that most atmospheric particles consist of no more than 50% soluble materials. The apparent decrease in the soluble portion with increasing particle size which was found by Fitzgerald et al. (1982) should not greatly decrease the ability of the particles to form droplets since the curvature effect decreases with increasing particle size. This makes droplet formation easier. As long as the soluble portion remains above 10%, activation should still occur. Also, an average soluble fraction of 50% is obviously sufficient to bring about the solute effect that overcomes the Kelvin effect for droplet formation.

1.7 Theory: Experimental Verification

Assuming that an atmospheric particle is composed entirely of soluble material allows the use of equation (1.6). For this relation, the critical supersaturation required by a particle for activation is dependent upon the size and chemical composition of the particle. If the particle size and the supersaturation are controlled, the chemical composition of the particle is the only remaining variable. It is a simple matter to control the particle size using a differential mobility analyzer. A known, stable supersaturation can also be provided by the use of a continuous flow diffusion cloud chamber. In such a chamber, the small, dry particles activate to form much larger droplets. With the proper experimental setup, it should be possible to determine the critical radius (r_c) and critical supersaturations (S_c) for actual CCN by introducing CCN into the system. The same can be done for known

materials which are suspected CCN components, such as ammonium sulfate and sodium chloride. By plotting r_c versus S_c measured for the actual CCN particles and the known materials, a direct comparison of the CCN behavior can be made. Similarities and differences between the plots could help to determine the behavior and composition of the CCN.

Perhaps the most difficult part of performing up this experiment was getting a source of actual atmospheric CCN particles. In this research, actual CCN were collected using cloud chamber apparatus which was recently built at the University of Missouri, Rolla (UMR) for a cooperative research project between the UMR and the Illinois State Water Survey. The large cloud chamber system was designed to separate out and capture actual CCN without any contamination from non-CCN particles. This was accomplished using a haze chamber, a cloud chamber, and several virtual impactors. With this apparatus, it was possible to capture the CCN particles on a filter. The water soluble portions of these particles were then extracted from the filter and injected into the air stream of the apparatus for this experiment. A brief description of the UMR apparatus and the experimental methods used will be given in the next chapter.

1.8 Summary of Thesis Research

The purpose of this research is to determine the chemical composition and behavior of cloud condensation nuclei. Chapter 2 describes the experimental setup and the methods used. Descriptions of cloud chamber theory and operation as well as of the UMR experimental apparatus are also included. Chapter 3 presents the results of the experiment. Chapter 4 summarizes the main points while drawing conclusions and offering recommendations for future work. Finally, a printout of the computer program that was written to control the cloud chamber as well as to collect the data from the optical particle counter is included in the Appendix.

1.9 References

Alofs, D. J.; Hagen, D. ; and Trueblood, M., "Measured Spectra of the Hygroscopic Fraction of Atmospheric Aerosol Particles," *J. Appl. Meteor.* 28, 126-136, 1989.

Andrews, E. and Larson, S. M., "Effect of Surfactant Layers on the Size Changes of Aerosol Particles as a Function of Relative Humidity," *Environ. Sci. Technol.* 27, 857-865, 1993.

Bigg, E. K., "Technique for Studying the Chemistry of Cloud Condensation Nuclei," *Atmos. Environ.* **20**, 75-80, 1986.

Bigg, E. K. , "Aerosol Over the Southern Ocean," *Atmos. Res.* **25**, 583-600, 1990.

Blanchard, D. C., "Sea-to-air Transport of Surface Active Material," *Science* **146,** 396-397, 1964.

Charlson, R. J. ; Vanderpool, A. H. ; Covert, D. S. ; Waggoner, A. P. ; and Ahlquist, N. C., "$H_2SO_4/(NH_4)_2SO_4$ Background Aerosol: Optical Detection in St. Louis Region," *Atmos. Environ.* 8, 1257-1267, 1974.

Charlson, R. J. ; Lovelock, J. E. ; Andreae, M. O. ; Warren, S. G., "Oceanic Phytoplankton, Atmospheric Sulphur, Cloud Albedo and Climate," *Nature* **326,** 655-661, 1987.

Cobourn, W. G. and Husar, R. B., "Diurnal and Seasonal Patterns of Particulate Sulfur and Sulfuric Acid in St. Louis, July 1977-June 1978," *Atmos. Environ.* **16,** 1441-1450, 1982.

Fitzgerald, J. W.; Hoppel, W. A.; and Vietti, M. A., "The Size and Scattering Coefficient of Urban Aerosol Particles at Washington, DC as a Function of Relative Humidity," *J. Atmos Sci.* **39**, 1838-1852, 1982.

Fitzgerald, J. W. and Hoppel, W. A., "Equilibrium Size of Atmospheric Aerosol Particles as a Function of Relative Humidity: Calculations Based on Measured Aerosol Properties," Hygroscopic Aerosols. L. H. Ruhnke and A. Deepak, Eds., Spectrum Press, 21-33, 1984.

Gill, P. S. and Graedel, T. E., "Organic Films on Atmospheric Aerosol Particles, Fog Droplets, Cloud Droplets, Raindrops, and Snowflakes," *Rev. of Geophys. and Space Phys.* **21,** 903-920, 1983.

Georgi, H. W., "Large-scale Spatial and Temporal Distribution of Sulfur compounds," *Atmos. Environ.* **12,** 681-690, 1978.

Hänel, G., "The Properties of Atmospheric Aerosol Particles as Functions of the Relative Humidity at Thermodynamic Equilibrium with the Surrounding Moist Air," *Adv. Geophys.* **19**, 73-188, 1976.

Harrison, L., "The Segregation of Aerosols by Cloud-Nucleating Activity. Part II: Observation of an Urban Aerosol," *J. Climate and Appl. Meteor.* **24,** 312-321, 1985.

Hinds, W. C., Aerosol Technology: Properties. Behavior, and Measurement of Airborne Particles. John Wiley & Sons, New York, 1982.

Husar, R. B. and Shu, W. R., "Thermal Analysis of the Los Angeles Smog Aerosol," *J. Appl. Meteorol.* **14**, 1558-1565, 1975.

Junge, C. E. and McLaren, E., "Relationship of Cloud Nuclei Spectra to Aerosol Size Distribution and Composition," *J. Atmos. Sci.* **28**, 382-390, 1971.

Ketseridis, G. and Eichman, R., "Organic Compounds in Aerosol Samples," *Pure Appl. Geophys.* **116,** 274-282, 1978.

Junge, C. E., "Our Knowledge of the Physico-chemistry of Aerosols in the Undisturbed Marine Environment," *J. Geophys. Res.* **77**, 5183-5200, 1972.

Meszaros, E., "On the Size Distribution of Water Soluble Particles in the Atmosphere," *Tellus* **20**, 443-448, 1968.

Monastersky, R. , "Cloudy Concerns," *Science News*, **136,** 106, 1989.

Ono, A. and Ohtani, T., "On the Capability of Atmospheric Sulfate Particles as Cloud Condensation Nuclei," *J. Rech. Atmos.* **14**, 235-240, 1980.

Rood, M. J. ; Hansson, H. C. ; Wiedensohler, A. ; and Covert, D. S. , "Experimental Determination of the Hygroscopic Properties of Organically Coated Aerosolä Particles," 84th Annual Meeting of the Air and Waste Management Association, Vancouver, British Columbia, Canada, 91-51.8, 8pp, 1991.

Rosinski, J. ; Gandruid, B. W. ; Nagamoto, C. T. ; and Parungo, F. , "Cumulative Chemical Composition of Atmospheric Cloud Condensation Nuclei,"/. *Aerosol Sci.* **15**, 709-718, 1984.

Seinfeld, J. H. , Atmospheric Chemistry and Physics of Air Pollution. John Wiley & Sons, New York, 1986.

Sekigawa, K., "Estimation of the Volume Fraction of Water Soluble Material in Submicron Aerosols in the Atmosphere," *J. Meteor. Soc. Japan* **61,** 359-366, 1983.

Twomey, S. and Severynse, G. T., "On the Relation Between Sizes of Particles and Their Ability to Nucleate Condensation of Natural Clouds," *J. Rech. Atmos.* **1**, 81-85, 1964.

Twomey, S. , "The Composition of Cloud Nuclei," *J. Atmos. Sci.* **28**, 377-381, 1971.

Twomey, S., "Measurements of the Size of Natural Nuclei by Means of Nucleopore Filters," *J. Atmos. Sci.* **29**, 318-321, 1972.

Twomey, S., Atmospheric Aerosols. Elsevier Scientific Publishing Company, Amsterdam, 1977a.

Twomey, S., "On the Minimum Size of Particles for Nucleation in Clouds," *J. Atmos. Sci.* **34**, 1832-1835, 1977b.

Twomey, S., "The Influence of Pollution on the Shortwave Albedo of Clouds," *J. Atmos. Sci.* **34**, 1149-1152, 1977c.

Twomey, S.; Piepgrass, M. ; and Wolfe, T. L., "An Assessment of the Impact of Pollution on Global Cloud Albedo," *Tellus* **36B**, 356-366, 1984.

Whitby, K. T., "The Physical Characteristics of Sulfur Aerosols," *Atmos. Environ.* **12**, 135-159, 1978.

Wigley, T. M. L., "Possible Climate Change due to S02-derived Cloud Condensation Nuclei," *Nature* **12**, 135-159, 1989.

Williams, A. L. ; Rothert, J. E. ; McClure, K. E. ; Alofs, D. J. ; Hagen, D. E. ; White, D. R.; Hopkins, A. R.; and Trueblood, M. B., "Determining the Chemical Composition of Cloud Condensation Nuclei- Third Progress Report," SWS contract Report 503, December, 1992.

Winkler, P., "The Growth of Atmospheric Aerosol Particles as a Function of Relative Humidity-Part II: An Improved Concept of Mixed Nuclei," *Aerosol Sci.* **4**, 373-387, 1973.

Chapter 2

Experimental Setup and Methods

2.1 Introduction and Chapter Summary

Several types of continuous flow diffusion cloud chambers have been designed over the years. This chapter presents the theory behind cloud chambers as well as a detailed description of the design chosen for this research. Also presented is a brief description of the experimental system at the University of Missouri, Rolla, which was used to capture the CCN tested in this research. Finally, the components of the system used for this research are discussed along with the experimental method.

2.2 Cloud Chamber Theory and Operation

Cloud chambers rely on diffusion to produce a continuous supersaturation (Twomey, 1977a). Both static and continuous flow diffusion chambers exist. Continuous flow diffusion (CFD) chambers expose a continuous stream (pulled through) of an aerosol to supersaturated conditions while allowing ample time droplet growth. On the other hand, static chambers only expose aerosol which naturally passes between their plates to supersaturated conditions. Since the CFD chamber design was chosen for this experiment, the static design will not be discussed. The basic apparatus for a CFD chamber is fairly simple. The detailed description of a typical chamber which is given in Twomey (1977a) is summarized here. The equations which are provided were originally developed for static diffusion chambers. Later work by Mahata et al. (1973) showed that the supersaturation in a CFD chamber will behave as in a static chamber as long as the actual centerline chamber air velocity is greater than a minimum value, V_c. The Mahata et al. (1973) research determined that this minimum velocity was necessary to prevent buoyancy-induced backflows near the hot plate of the chamber. These backflows would result in a thermal cell forming inside the cloud chamber. V_c can be calculated for a CFD using

$$V_c = 0.43(T_h - T_c)d^2 \qquad (2.1)$$

where,

V_c = minimum centerline velocity in the chamber [cm/s]
T_h = hot plate temperature [° C]
T_c = cold plate temperature [° C]
d = plate spacing [cm]

Using this equation, the V_c for the chamber used for this experiment was found to be 1.72 cm/s. The actual center line velocity was set at 6.4 cm/s. Thus, this condition is satisfied and the supersaturation equations from Twomey (1977a) can be used.

A thermal diffusion chamber achieves supersaturation by providing two wet, parallel plates which are held at different temperatures. These temperatures can be represented by T_c for the cold plate and T_h for the hot plate. Air which passes through the chamber is continuously saturated by diffusion of water vapor from the wet surfaces. As the air sample flows between the plates, the local temperature, T, and the water vapor density become linearly proportional to the distance from the cold plate. Vapor density, p_v, is related to the saturation vapor pressure, p_s, by the ideal gas law. The relation is

$$\rho_v = \frac{M p_s}{R\Theta} \qquad (2.2)$$

where,

M = molecular weight of the liquid
R = ideal gas constant
0 = absolute temperature

The local vapor density is therefore also linearly proportional to local temperature. This is represented by line ADB in Figure 2.1. The equilibrium vapor density is represented by the curved line ACB. The equilibrium vapor density, p_s, of water at temperature 0 follows the theoretical Clausius-Clapeyron relationship:

$$\frac{1}{\rho_s}\frac{d\rho_s}{d\Theta} = \frac{M_w L}{R\Theta^2} - \frac{1}{\Theta} \qquad (2.3)$$

where,

M_w = molecular weight of water
L = latent heat of condensation of water

Points A and B in Figure 2.1 represent the cold plate and the hot plate respectively. At the plate surfaces, the local and equilibrium vapor densities are equal and the relative humidity is 100%. Since the equilibrium vapor pressure response is parabolic instead of linear, the actual vapor density between the two surfaces exceeds the equilibrium value for the prevailing temperature. The supersaturation which is achieved is defined as the difference between the local and saturation vapor densities divided by the saturation vapor density. The supersaturation for Figure 2.1 is therefore represented by the line segment ratio CD/CE. Varying supersaturations are achieved by varying the temperatures of the wet surfaces.

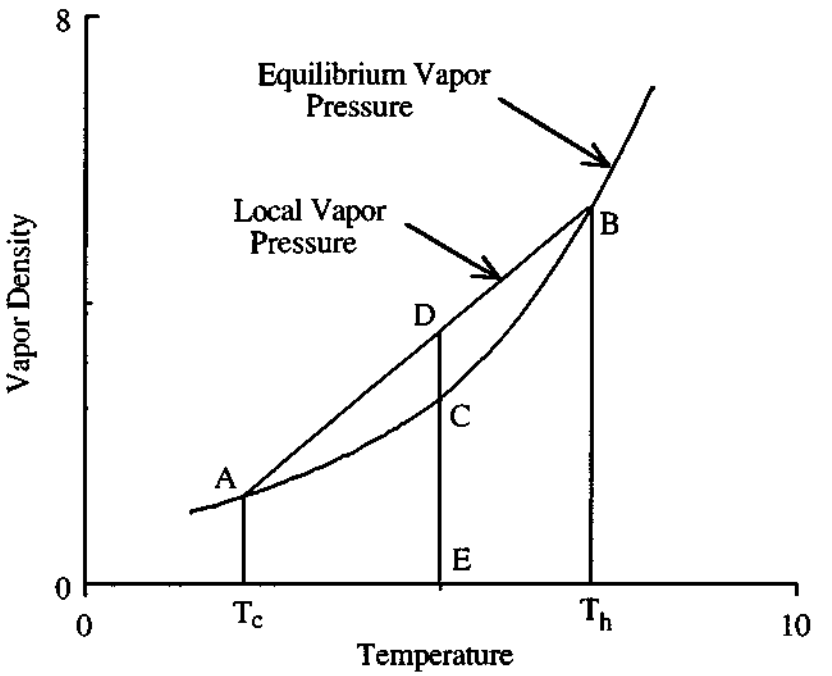

Figure 2.1: Vapor Pressure in a Thermal Diffusion Chamber

For most cloud chamber designs, the two plates are spaced 1 cm apart and are kept at a temperature difference in the range of 2° to 8° C (Twomey, 1977a). An equation relating the supersaturation achieved to the temperature difference of the plates was derived

for a horizontal plate setup by Twomey (1977a) considering the steady-state diffusion of water vapor. The final equation is as follows:

$$S(z,\Theta_1,\Theta_2) = \frac{z}{h}\left(1 - \frac{z}{h}\right)(\Theta_2 - \Theta_1)^2\left[\frac{1}{2}\left(\frac{M_w L}{R\bar{\Theta}^2} - \frac{1}{\bar{\Theta}}\right)^2 - \frac{M_w L}{R\bar{\Theta}^3} + \frac{1}{2\bar{\Theta}^2}\right] \qquad (2.4)$$

where,

z = height from bottom (cold) plate in chamber
h = height of top (hot) plate from bottom plate
M_w = molecular weight of water
L = latent heat of condensation
R = ideal gas constant
Θ_1 = temperature of bottom (cold) plate (z = 0) in K
Θ_2 = temperature of the top (hot) plate (z = h) in K

$\bar{\Theta}$ = mean absolute temperature of the two plates

This equation gives the maximum supersaturation attained in the chamber. A more detailed discussion of the derivation of this formula is presented in the work by Twomey (1977a). Figure 2.2 shows a plot of the theoretical maximum supersaturation attained within a given CFD chamber as a function of the temperature difference as calculated by Equation (2.4). The maximum supersaturation occurs midway (h/2) between the two plates, with the supersaturation dropping off parabolically towards the plate surfaces (Twomey, 1977a). This difference in supersaturations across the chamber is usually ignored since the velocity profile between the plates is also parabolic, thus allowing more time for droplet growth in the regions of lesser supersaturations (Williams et al., 1992). For this experiment, the particles were collected midway between the plates in an attempt to sample only those particles which have been exposed to the maximum supersaturation, thereby reducing any errors. Equation (2.4) is used for this experiment to calculate the maximum supersaturations based on the temperature difference but for a vertical plate alignment. Since a small, visually aligned sampling tube inserted between the cloud chamber plates must be used to obtain data with this experiment, the parabolic drop in supersaturation across the diameter of the sampling tube could cause a small error. In order to reduce error

an average supersaturation over the tube will be used instead of the maximum value. The chamber used has a spacing of h = 1 cm, so S_{max} occurs at z = 0.5 cm. The sampling tube inner diameter is 0.25 cm. The inner edge of the aluminum sampling tube is located at z = 0.5 - (0.25/2) = 0.375 cm. An average value for the supersaturation across the area of the tube can be calculated to be 97% of S_{max}. The conversion is therefore $S_{aVg} = 0.97S_{max}$.

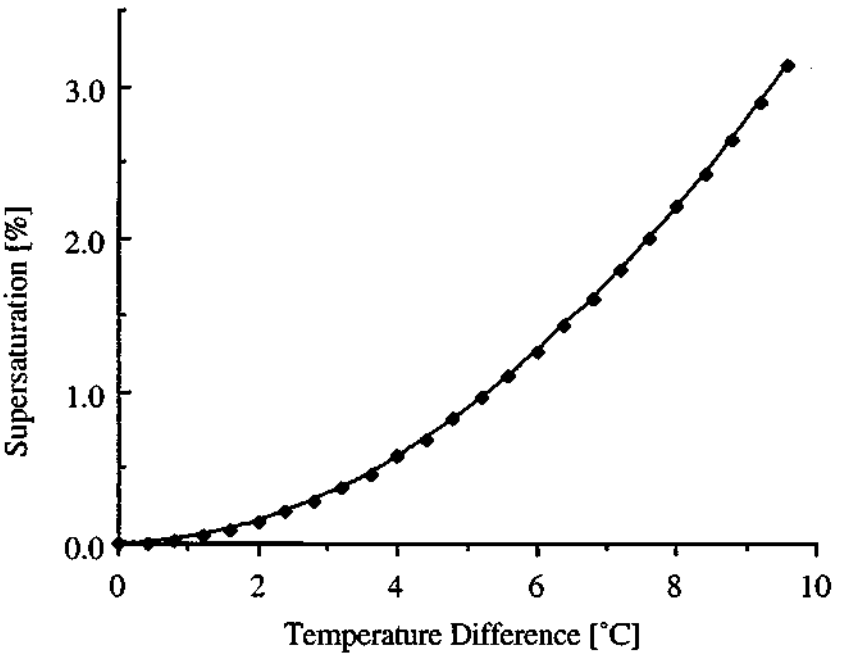

Figure 2.2: Supersaturation In a Thermal Diffusion Chamber as a Function of Temperature Difference (as calculated by Equation (2.2))

2.2.1 Selected Cloud Chamber Design

The design which was chosen for this experiment is a continuous flow diffusion (CFD) chamber with vertical plate orientation (Figure 2.3). The two vertical surfaces are provided by two aluminum boxes. These boxes are set parallel to one another 1 cm apart. Each box is 1.22 meters long, 15 cm wide, and 5 cm deep. They both provide a wetting

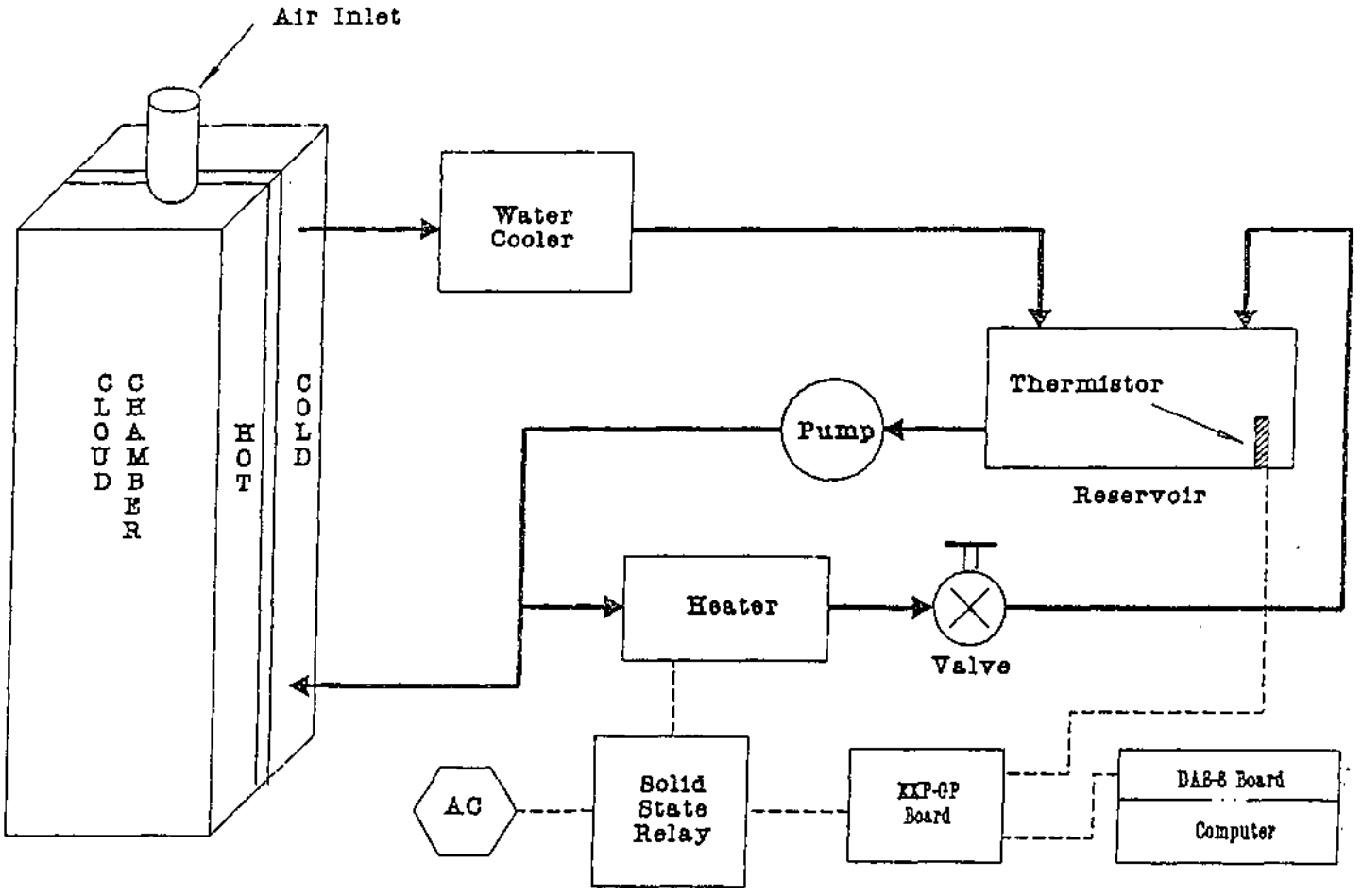

Figure 2.3: Water Flow Diagram for Temperature Control of the Cold Plate of the CFD Chamber. (A separate, identical system exists for the temperature control of the hot plate. Heavy lines indicate water system tubing, while dashed lines indicate electrical connections between instruments.)

surface which is 1.20 meters long and 13 cm wide. The 1 cm gaps along the sides of the chamber are sealed with O-ring tubing to prevent leaks. After construction, the chamber was leak tested to ensure that no contamination of the samples or the data would occur. The two inner surfaces of the chamber are kept wet by running deionized water down wicking paper which is held to the chamber surfaces. This paper is kept wet at all times by a gravity feed of deionized water. The excess water is pumped from the bottom of the chamber, filtered, and fed back into the wetting system.

2.2.2 Temperature Control

The temperatures of the two cloud chamber surfaces are regulated by flowing water at individually controlled temperatures through the aluminum boxes. The aluminum sheeting that makes up the boxes quickly equilibrates to the temperature of the water. The temperature of the water itself is controlled by the computer program which was written to control all aspects of the cloud chamber operation and data collection. To set the surface temperatures, the operator inputs the desired values into the computer. The computer then sends signals to devices which heat and cool the water as necessary to maintain these set temperatures.

Figure 2.3 shows a diagram of the water flow necessary for the temperature control of a single chamber surface. The solid bold lines represent the tubing for the water flow. The dashed lines indicate connections between electronic components. Two identical systems exist for the cloud chamber, one for the hot plate and one for the cold plate. As shown in the diagram, a thermistor is located in the reservoir which reads the temperature of the water and sends a signal back to the computer via the Keithley Metrabyte EXP-GP access board and the Keithley Metrabyte DAS-8PGA analog input board. If this temperature is below the set temperature, the computer will send 5 volts to the solid state relay which then turns on the electric heating element. This heating element is a standard 1500W, 120V electric water heater element. The water that is pumped past the heater is

continually heated until the temperature in the reservoir is above the set point. Once this occurs, the computer stops sending a voltage to the solid state relay which turns off the heating element. Not all of the water in the system is pumped past the heating element. Only a small portion (about 25%) of the water flow must pass the heater to keep the water at the set temperature. The exact amount of water that is directed past the heater is controlled by a hand valve. The rest passes through one of the boxes of the cloud chamber. The water enters from the bottom of the aluminum box and exits out the top. This ensures that the box remains full of water at all times. Once the water has passed through the cloud chamber, it is cooled by a water cooler. The cooler is necessary for two reasons. First, it compensates for the extra heat which is put into the system by the water pump. Second, it dampens the response of the system to the heater input. In other words, the temperature slowly rises to the desired level instead of shooting past it. Even with this dampening, the temperature difference of the chamber does still fluctuate approximately 0.1 ° C after it has equilibrated.

2.2.3 Preventing Transient Supersaturations

The development of Equation (2.4) assumed fairly ideal conditions for the operation of a CFD cloud chamber. A theoretical analysis of non-steady state supersaturation distributions in a CFD chamber by Fitzgerald (1970) showed that transient supersaturations can occur near the inlet of a chamber. These transient supersaturations can occur near the hot plate if the incoming sample air is saturated at a temperature lower than the hot plate. Fitzgerald's (1970) calculations indicate that short lived supersaturation peaks which are several times greater than the maximum steady-state supersaturation are possible. This occurs because the diffusivity of water vapor in air is greater than the thermal diffusivity of air (Fitzgerald, 1970). As a result, the water vapor density reaches its linear steady-state distribution faster than the temperature can. Thus, the temperature is colder than it should be at that vapor density. This results in a higher humidity (i.e., a supersaturation). Saxena

et al. (1970) confirmed Fitzgerald's findings. This deviation could result in considerable error when taking data with a CFD cloud chamber. The transient super-saturations would result in the activation of particles at lower than expected supersaturation settings, thus biasing the data.

In order to prevent experimental errors due to transient supersaturations for this experiment, the typical cloud chamber design was modified. Since the transient supersaturations occur when the air sample enters the chamber at a temperature below the hot plate temperature, raising the sample air temperature to the hot plate temperature should remove the problem. It is necessary to raise the air temperature before it contacts wet surfaces in the cloud chamber. Mahata et al. (1973) determined that this could be accomplished by providing an initial length of the hot plate which is dry. This was provided by covering a portion of the wicking paper on the hot plate at the entrance of the chamber with aluminum foil. The foil traps the moisture from the wicking paper between itself and the hot plate while letting heat from the hot plate pass through it into the sample air. The necessary length of aluminum foil required was calculated based on the time needed for temperature equilibration. The sample air velocity was known, and the air temperature and hot plate temperatures were assumed to be 22 ° C and 30 ° C, respectively (worst case conditions). The calculations indicated that the aluminum foil must extend 15 cm down the length of the chamber from the inlet. This length also satisfied the requirement developed by Mahata et al. (1973) of a dry length greater than or equal to 15 times the plate spacing of the chamber (15 cm for this chamber). The presence of the foil somewhat reduces the amount of time droplets have to grow in the chamber but not enough to prevent their growth to an optically countable size.

2.3 CCN Capture at UMR

Since the research presented here was performed under the direction of Dr. Williams, a UMR collaborator, CCN samples collected by the UMR setup were made

available for study. The experimental setup at UMR is unique due to its purpose and scale. Previous studies of CCN chemical composition considered all CCN simultaneously. The system at UMR and its mobile cousin at the Illinois State Water Survey (ISWS) were designed to collect large ($0.1 < d_p < 0.5$ urn) and small ($d_p < 0.1$ µ m) CCN separately. This is necessary to get an accurate determination of CCN chemistry since large CCN are far less numerous than the small CCN but make up a majority of the total mass. The systems at UMR and the ISWS were also designed to collect much larger sample masses than ever before in order to facilitate sample analysis.

2.3.1 Experimental Setup

The CCN collection system at UMR consists of three virtual impactors, two CFD cloud chambers, and three filters (Williams et al., 1992). The virtual impactors are used to separate particles in the air sample according to their size. The particles are separated by their inertia, with the smaller particles passing on through the "fine flow" and the larger particles being removed in the "coarse flow". For the UMR system, samples of atmospheric air are initially passed through an impactor which allows only particles smaller than 0.5 µ m to pass (Williams et al., 1992). This is done since this experiment is mainly interested in CCN smaller than this size. Allowing larger particles to enter the system would increase the chances of the small CCN sample being contaminated by the presence of the much larger atmospheric particles. The particles smaller than 0.5 µ m are then passed through a large haze chamber, which is a CFD chamber held at 100% Relative Humidity.

Inside the haze chamber, hygroscopic particles in the air stream grow to become droplets. The equilibrium size (x_o) of these droplets at 100 % RH depends only on the S_c of the particle (Laktionov, 1972; Williams et al., 1992). The relation developed by Laktionov is $x_o = 0.08/S_c$, with x_o in µ m and S_c in percent. The humidified air is then passed through a second virtual impactor which removes the newly formed droplets which are larger than 0.5 µ m in diameter. By the Laktionov relation, the S_c corresponding to

x_o = 0.5 µm is 0.16% (Williams et al., 1992). Thus for hygroscopic particles, only particles with Sc > 0.16% will pass through the fine flow of the second impactor. The droplets which enter the coarse flow are captured on either a quartz or a glass filter. The sample on this filter represents the large CCN.

The droplets which are smaller than 0.5 urn along with the particles which were not nucleated are then passed through a large CFD cloud chamber which is kept at a supersaturation of 0.95% (Williams et al., 1992). This supersaturation is approximately equal to the maximum supersaturation level of 1% found in naturally occurring clouds. Inside of the CFD chamber, all of the particles with an S_c < 0.95% will activate to form droplets. Particles with S_c > 0.95% will most likely be unable to activate under natural conditions and thus can be ignored. The supersaturated air stream is then passed through a third impactor with a cut-point of 1.0 urn. This impactor removes the droplets which have grown to a size larger than 1.0 µm in diameter. These droplets are collected on a filter and represent the small CCN (Williams et al., 1992). The droplets smaller than 1.0 µm and the particles which do not activate pass out of the system through the pump. After sampling, the water remaining on each filter is allowed to dry, leaving behind the soluble and insoluble portions of the CCN.

2.3.2 CCN Sample Extraction

Before the CCN from the UMR research could be used for this study, it had to first be extracted from the filters. Samples were provided on two types of filters. Early samples were collected on 8.5 by 11 inch fiberglass filters, while later samples were collected on round quartz filters which were 47 mm in diameter. The reason for the filter switch was to allow for a more concentrated sample to be collected. This made extraction easier. The two different filter types each required their own method of CCN sample extraction. For the glass filters, their large size posed the greatest problem. This was overcome by carefully folding the filters and placing them in a small beaker containing

150 ml of double-distilled (DD) water. The filters were then agitated, while still in the DD water, for 72 hours in order to dissolve as much of the CCN sample as possible. The liquid in the beaker was then removed and pulled through a 0.4 µm millipore filter. The millipore filter was used to ensure that no contamination occurred from glass fibers that might have broken off of the filter.

The small size of the quartz filters allowed for the use of a different method of extraction. First, a clean 47 mm nucleopore filter was placed in a filter holder. The loaded quartz filter was then placed on top of this filter with the sample side up. Then another clean nucleopore filter was placed on top. The filter holder was then sealed, sandwiching the loaded filter between the two nuclepore filters. The purpose of the nucleopore filters is to prevent particulate material from entering and contaminating the sample. After the filters were positioned, a 20 cc syringe containing 20 ml of deionized (DI) water was attached to the inlet of the filter holder. A collection bottle was then attached to the outlet of the filter holder. Once the bottle was in place, 10 ml of the DI water was injected through the filter. Of this 10 ml, usually only 5 ml passed through the filter. The other 5 ml remained in the filter. Then the entire apparatus was placed in an ultrasonicator for 16 minutes (the maximum retention time of the device). Half way through the 16 minutes, another 5 ml of DI water was injected from the syringe through the filter. At the end of the sonication period, the remaining 5 ml were injected. Then, in an attempt to extract as much water as possible from the filter, a small amount of air was passed through the filter using the syringe. Finally, another 20 ml of DI water was passed through the filter holder in order to remove any remaining soluble portions of the CCN sample. Both of these extraction methods liberate only the soluble portion of the CCN samples, leaving the insoluble portions on the filters. Any attempt, however, to remove the insoluble portion of the CCN would have required great effort and may have resulted in contamination of the sample. An accurate representation of the soluble portion of the CCN should still have been attained with the present methods. Thus, the only direct results of this research are for the soluble

portion of the CCN. All of the CCN sample extractions for this experiment were performed by Jane Rothert of the ISWS.

2.4 CCN Particle Generation

To perform this experiment, it is necessary to provide a continuous stream of dry CCN particles. Since the CCN samples are in solution after they are extracted from the filters, a device is required which can produce dry particles from a dilute solution. There are many such instruments on the market. The one which was chosen for this experiment is the TSI Model 3460 Tri-Jet Particle Generator. This device atomizes a stream of any solution placed in one of its three atomizer jars using a high-velocity jet. This produces small droplets of solution which are drawn out of the atomizer jar by a pump. These droplets are then dried with a desiccant tube style diffusion dryer. Removing the water from the droplets leaves behind the soluble, nonvolatile materials that were in the solution, resulting in the production of a polydispersion of dry particles. This instrument was also used to produce particles of known composition, such as ammonium sulfate. This was easily accomplished by placing a solution made from deionized water and a small amount of the desired salt in one of the generator's solution containers. Figure 2.4 shows a diagram of the orientation of this instrument as well as all of the instruments discussed in sections 2.5 through 2.7. Refer to this figure for assistance in understanding the experimental setup as discussed throughout Chapter 2.

2.5 Particle Size Selection

As stated in section 1.7 , it is necessary to know the size of the dry particles which are nucleated at a given supersaturation to be able to examine their behavior. Therefore, a method of selecting a monodispersion of a known size from the polydispersion produced by the particle generator is required. To do this, the polydispersed air stream is passed through a Differential Mobility Analyzer (DMA), also known as a Classifier. This

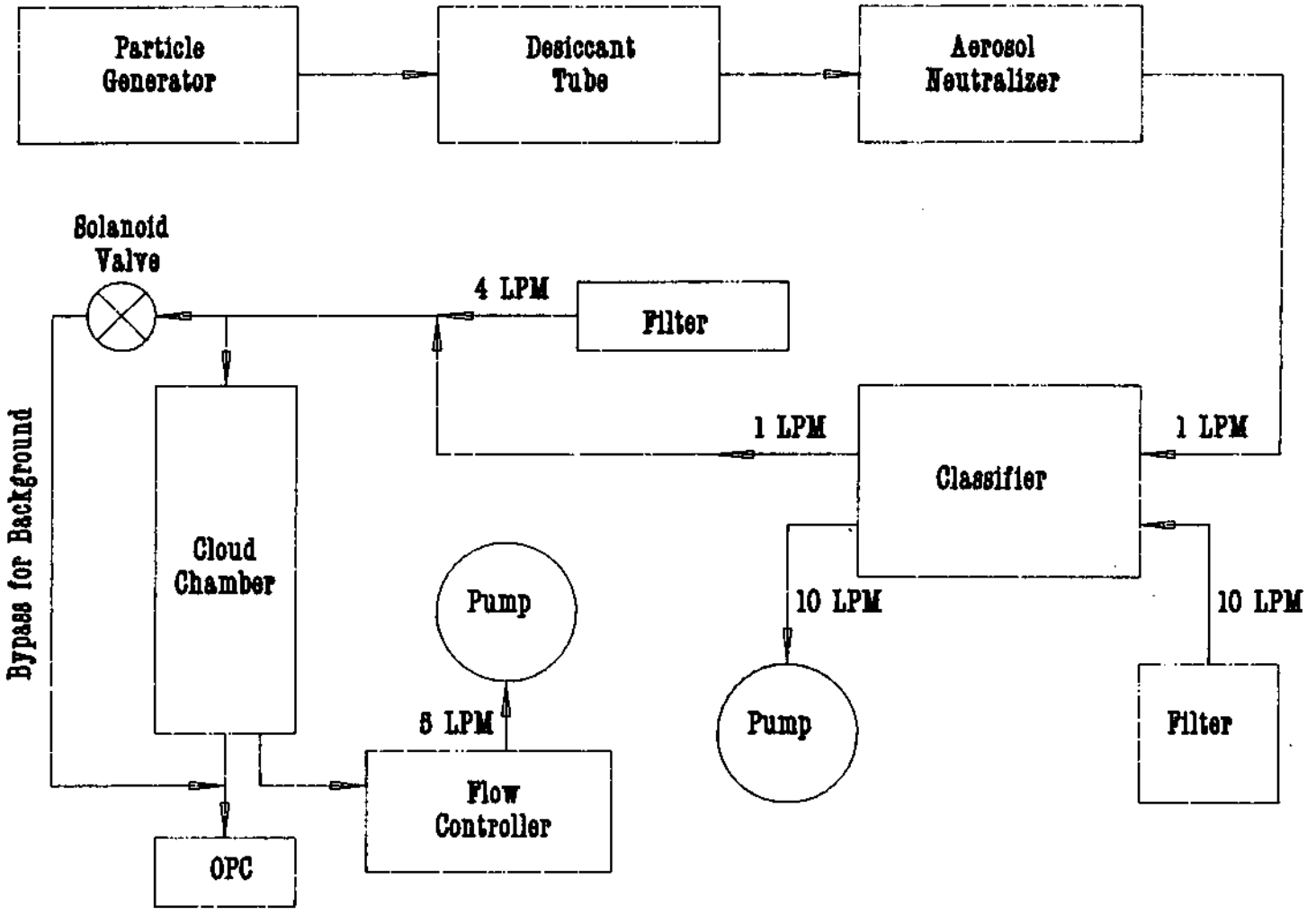

Figure 2.4: Airflow Schematic for Experimental Apparatus
(Arrows indicate direction of flow)

instrument separates particles according to their mobility in an electric field. First, the particles are passed through a Kr-85 aerosol neutralizer, which establishes a bipolar-equilibrium charge level on the particles. The particles then enter the sample stream of the Classifier. The electric field which is produced by the voltage across the Classifier attracts the positively charged particles, causing them to pass through a sheath of filtered air toward a collection slit. Only particles of a certain mobility pass through the slit. Particles with too large a mobility (smaller size) do not reach the slit as they are impacted on a center electrode. Particles with a mobility less than that which is required by the voltage setting will not be drawn far enough through the sheath air to be collected. The selected monodisperse size is easily changed by changing the voltage across the Classifier. The Classifier which was used for this experiment was built by UMR based on the design of the TSI Model 3071 Electrostatic Classifier.

The sizes which were most often selected for the Classifier for this experiment ranged from 0.01 (the lower limit of the Classifier) to 0.05 um in diameter. It should be noted that the particle diameters selected for the examination of the CCN behavior were not necessarily equal to the original CCN dry diameters. This is not a problem, however, since this research is concerned with determining the CCN material and its behavior rather than actual particle size.

2.6 CCN Activation in the CFD Cloud Chamber

After a monodispersion is selected from the CCN particles, the sample air can be passed through the cloud chamber. The sample air flow rate of 11pm which is produced by the Classifier is combined with 41pm of filtered air just before it enters the top of the cloud chamber. This is done so that the cloud chamber flow rate can be set at 5 1pm. The flow rate of the system was originally controlled by a Kurz Model 251 Constant Flow Air Sampler which was in turn controlled by the computer program. Due to mechanical difficulties with this instrument, later samples were collected using a simple manual valve

to ensure a flow rate of 5 lpm. This flow rate resulted in a chamber velocity of 6.4 cm/s. The total chamber length from the inlet to the inlet of the sampling tube was 110 cm. Thus, there was a total residence time for the air in the chamber of 17.2 seconds. The droplets were not exposed to supersaturated conditions for the entire time, however. Air entering the chamber initially spent 2.3 seconds in the aluminum foil region in order to prevent transient supersaturations. Once past this region, a supersaturation could to develop. It did not, however, develop instantaneously. The time required was equal to the square of the chamber plate spacing (1 cm for this chamber) divided by the diffusion coefficient of water vapor at the operating temperature (0.25 cm^2/s for this chamber). Thus, for this chamber, 4 seconds were required for supersaturation development. Therefore, 10.9 seconds remained for the droplets to form and grow on the CCN inside the chamber. For this study, the supersaturation of the cloud chamber ranged from around 0.35% to 0.55%. These settings were more than sufficient to allow for activation of the captured CCN particles.

2.7 Droplet Data Collection

After the sample air had passed through the cloud chamber, it was necessary to determine whether or not droplets formed on the CCN particles. To do this, a device which could count and size the droplets was needed. The Particle Measuring Systems (PMS) Model ASASP-X optical particle counter (OPC) was selected to perform this task. This OPC uses a He-Ne laser to size and count particles based on their light scattering properties. This particular model of the PMS OPC has 32 size channels ranging from 0.09 µm to 3.0 µm in diameter. The minimum size range of the OPC does prevent direct counting of the CCN particles in their dry state. Since the main area of concern is the critical supersaturation which results in the activation of the CCN particles and not the number or size of the dry particles themselves, this restriction presents only a minor problem.

The OPC was set up so as to collect the sample at a point inside of the cloud chamber just above the chamber exit. This was done by inserting a piece of 1/8 inch aluminum tubing through a fitting in the bottom of the chamber. The inlet of the OPC was attached to the external end of the aluminum tube. The tube extended 10 cm into the chamber and was positioned so that its opening was in the center of the gap between the two plates. This provided sampling at the point of maximum supersaturation. A "T" fitting was also attached to the aluminum tube. This was done so that a tube could be joined to the OPC from a point prior to the chamber inlet. This tube, which shall be referred to as the "background" tube, allows for data collection of the sample air without activation of the particles. The flow of sample air through the background tube is controlled by a solanoid valve which is in turn controlled by the computer. The valve is only opened during the times that the cloud chamber temperatures are being equilibrated. During droplet sampling the valve is closed. This sampling of the background air also has the added benefit of keeping the sampling tube dry and clear of obstructions. The operation of the OPC was controlled by the computer program which was written for this project. The data collected by the OPC were sent directly to the computer for real-time viewing and storage.

2.7.1 Droplet Identification

In order to obtain useful data from the OPC, a reliable method was needed to determine whether droplets had formed on the CCN particles. The monodisperse sizes selected from the polydispersions of CCN particles were all smaller than the lower limit of the OPC. This prevented direct measurements of the CCN particles in the background air (CCN laden air not passed through the CFD chamber). Since the CCN particles were the only ones expected in the background air, zeros in all the channels of the OPC was reasoned to be correct. The presence of any particles in the background air which could be counted by the OPC would have been an indication of contamination of the sample by a leak. Counting the droplets in air from the CFD chamber would indicate the presence of

activated CCN. The sample air had a residence time of 10.9 seconds in the supersaturated region of the CFD chamber. During this time period, CCN particles grow from a few hundredths of a micrometer to several micrometers in diameter. These relatively large droplets were easily counted by the OPC and indicated their presence by showing counts in the upper eight channels. Counts in these channels, which correspond to a size range of 1.21 urn to 3.0 µ m, could only be produced by the presence of droplets formed on the CCN particles. Thus, the identification of droplet formation is a simple matter. In summary, first the background particle stream is sampled by the OPC to check for any contamination. If none is found, the air from the CFD chamber is sampled, and the presence of counts in the upper channels of the OPC for the supersaturated air sample indicates activation has occurred.

2.7.2 Droplet Growth

In order to obtain accurate data, the droplets exiting the CFD chamber had to be large enough for the OPC to differentiate between them and any particles which might not have been activated at the supersaturation present in the chamber. To do this, the final sizes of the droplets formed for each of the supersaturations studied were calculated using the droplet growth equation. Once a particle is activated, droplet growth is driven by the difference between the environmental vapor pressure and the equilibrium vapor pressure. The equilibrium value tends to decrease with increasing droplet radius, which increases the condensation rate. All of these factors are considered in the droplet growth equation (Fletcher, 1969), which is

$$r\frac{dr}{dt} = G\left(S - \frac{a}{r} + \frac{b_N}{r^3}\right) \qquad (2.5)$$

where,

$$G = \frac{D\rho_v}{\rho_L}\left[1 + \frac{DL^2\rho_v M_0}{RT^2\kappa}\right] \qquad (2.6)$$

and,

r = radius of the droplet
dr/dt = growth rate of the droplet
S = supersaturation
a = curvature term (see Equation (1.4))
b_N = solute term (see Equation (1.5))
D = diffusion coefficient of water vapor
L = latent heat of vaporization of water (per gram)
M_o = molecular weight of water
R = ideal gas constant
T = absolute temperature
p_v = density of water vapor in the environment
PL = density of liquid water
K = thermal conductivity of air

The variables in Equation (2.5) can be separated and integrated analytically. An easier way to use this relation is to simplify the equation by dropping the solute term, (b_N/r^3). Since the nucleus of the droplet being considered is activated, the curvature term is already dominant over the solute term (Twomey, 1977a). Thus, dropping the solute term introduces little error (less than 1%). It is also often possible to drop the curvature term, (a/r), without introducing serious error (less than 1 %). This is true as long as $| a/r | \leq 10^{-3}$, which holds for droplets 1 μm or larger (Twomey, 1977a). With these simplifications, Equation (2.5) becomes

$$r \frac{dr}{dt} = GS \qquad (2.7)$$

which can be integrated to yield the relation

$$r^2 = 2GSt \qquad (2.8)$$

Equation (2.8) was used to calculate the size of the droplets formed in the CFD chamber at the four supersaturations at which it was operated. The growth time, t, for all of the sampling runs was 10.9 seconds. The value of G, calculated for an average temperature of 27 °C, was 1.372×10^{-6} cm^2/s. The droplet diameters which were obtained are provided in Table 2.1.

Table 2.1: Drop Diameters at the Exit of the CFD Chamber

ΔT [° C]	Supersaturation [%]	Drop diameter [um]
3.2	0.354	6.51
3.5	0.423	7.11
3.75	0.485	7.62
4.0	0.550	8.11

These calculations indicate that the droplets will grow to diameters several times larger than the OPC upper limit of 3.0 μm. These are the diameters reached prior to the droplets entering the sampling tube. The sampling tube, which is 25 cm long (10 cm of which is inside the CFD chamber), is not kept at a supersaturation. This results in a decrease in supersaturation in the air inside the tube. Once the relative humidity drops below 100% (0% supersaturation), the droplets begin to shrink due to evaporation. The flow rate in the tube was 1.5 cm^3/s. This resulted in a residence time of 0.85 seconds for the sample tube. During this time, the evaporation brought the droplets within the upper end of the OPC range for all of the samples tested. The reduction in size was not, however, sufficient to cause problems with determining which counts were dry particles and which were droplets. This shows that particles registered in the upper OPC channels are activated droplets and not non-activated particles. Since the supersaturation at which droplet formation occurred was the only necessary data, the droplet size fluctuations due to partial evaporation in the sampling tube posed no problems.

2.8 Overall Air Flow Setup

A schematic of the overall airflow of the system is shown in Figure 2.4. The CCN particles were produced by the particle generator. A monodispersion of particles of a known diameter were then selected by the Classifier. This sample of particles was then either passed through the CFD chamber or bypassed directly to the OPC for background data collection. The OPC then sent the data to the computer for viewing and storage. The

flow of the air through the system was controlled by two pumps, a solanoid valve, an electronic flow controller (later replaced by a manual valve), and the computer program.

2.9 Critical Supersaturation Determination Method

As mentioned previously, the critical supersaturation (S_c) of the CCN particles corresponding to a given size is the determining characteristic for the comparison of the particles' behavior to that of particles of known composition. One possible way to use the experimental apparatus to find the S_c for a known r_c would have been to hold the particle size at a single value while raising the supersaturation in the cloud chamber. This would have been repeated until activation occurred and droplets were counted. This, however, is not a practical method since the CFD chamber temperatures require approximately 20 minutes to come to equilibrium after each change in the desired temperature difference. An alternative method was to hold the CFD chamber at a constant supersaturation while increasing the size of particles passing through the chamber. The response of the Classifier to a change in voltage is almost immediate. Thus, it was possible to increase the voltage (i.e., increase the particle size) and wait approximately 1 minute to see if counts appeared in the upper channel of the OPC data. This process was repeated until droplets appeared. The particle radius corresponding to the voltage across the classifier was then recorded as the value of r_c and the supersaturation in the CFD chamber as its corresponding S_c. This process was performed for all of the CCN samples and known material samples at four different supersaturations. Results from these experiments are discussed in Chapter 3.

2.10 References

Fitzgerald, J. W., "Non-Steady State Supersaturations in Thermal Diffusion Chambers," *J. Atmos. Sci.* **27**, 70-72, 1970.

Laktionov, A. G., "A Constant Temperature Method of Determining the Concentrations of Cloud Condensation Nuclei," *Atmos. Ocean Phys.* **8**, 382-385, 1972.

Mahata, P. C.; Alofs, D. J.; Sinnarwalla, A. M., "Supersaturation Development in a Vertical-Flow Thermal Diffusion Chamber," *J. Appl. Meteor.* **12**, 1379-1383, 1973.

Saxena, V. K. ; Burford, J. N. ; and Kassner Jr., J. L., "Operation of a Thermal Diffusion Chamber for Measurements on Cloud Condensation Nuclei," *J. Atmos. Sci.* **27**, 73-80, 1970.

Twomey, S., Atmospheric Aerosols. Elsevier Scientific Publishing Company, Amsterdam, 1977 a.

Williams, A. L. ; Rothert, J. E.; McClure, K. E. ; Alofs, D. J. ; Hagen, D. E.; White, D. R.; Hopkins, A. R.; and Trueblood, M. B., "Determining the Chemical Composition of Cloud Condensation Nuclei- Third Progress Report," SWS contract Report 503, December, 1992.

Chapter 3

Results and Discussion

3.1 Introduction and Chapter Summary

This section presents measurements of the critical supersaturation versus critical radius for three actual CCN samples as well as laboratory-generated aerosols of NaCl and $(NH_4)_2SO_4$ The dry (unactivated) CCN sizes corresponding to the voltage settings of the Classifier were determined. The reproducibility of the CCN data was confirmed, and the critical supersaturation and radius of the CCN were compared to those of NaCl and $(NH4)_2SO_4$. These data were then used to calculate Ω, the number of ions per unit volume formed by dissolution of the CCN in the activated droplets. The value of Ω depends only upon the composition of the dry particle material. The Ω values obtained for the CCN samples were compared to the Ω values corresponding to NaCl and $(NH_4)_2SO_4$. This comparison pointed to ammonium sulfate as the component of the large CCN samples which controlled the activation characteristics of the particles. The results of preliminary chemical analyses of the CCN samples which were tested are also presented. These analyses indicated that the large CCN samples contained 63.3 % ammonium sulfate, 32.2 % organic compounds, and 4 % elemental carbon. These results were used to calculate Ω for the soluble organics present in the CCN samples. The value of the Ω term for the organics indicated that these compounds are significantly less active than ammonium sulfate.

3.2 Verification of Operation

In order to ensure correct experimental results, it was first necessary to verify the operation of key pieces of equipment in the system. The instruments of greatest concern were the Classifier and the CFD chamber. Deviations in the performance of either of these pieces of equipment would have resulted in errors in the critical supersaturation versus critical radius data sets. Therefore, it was necessary to check their calibration. The

computer program which controlled the temperature difference of the CFD chamber was written to prevent deviations of more than 0.1 ° C from the temperature set for either plate. If both plates deviated from their set temperatures by this amount in opposite directions (an error of 0.2 ° C), the error in the supersaturation obtained in the CFD chamber would be approximately 9% (using Equation (2.4)). Observations of the individual plate temperatures during the operation of the CFD chamber showed that after equilibration the temperature deviation seldom reached 0.1 ° C. The sum of the two deviations usually remained at or below 0.1 ° C. This deviation would result in an error in the supersaturation of approximately 4.7% of the total value. Thus, a supersaturation of 0.5 % would have had an error of plus or minus 0.0235 %.

The temperature differences between the plates of the cloud chamber for this experiment are presented in Table 3.1 along with their corresponding supersaturations. The maximum supersaturations were calculated using Equation (2.4). The "averaged" supersaturations, which were used in later calculations, were found using the relation $S_{avg} = 0.97 S_{max}$ (as discussed in section 2.2).

Table 3.1: CFD Chamber Supersaturation Settings

ΔT [° C]	Smax [%]	Savg [%]
3.2	0.365	0.354
3.5	0.436	0.423
3.75	0.500	0.485
4.0	0.567	0.550

3.2.1 Classifier Calibration

The Classifier, which was provided by UMR, came with a calibration data set. Initially, this calibration was assumed to be correct. However, preliminary runs of the apparatus showed a slight deviation from expected particle sizes. Therefore, it was necessary to perform a second calibration linking Classifier voltage to particle size. This was done using the particle generator, the CFD chamber (already calibrated) and the OPC.

The particle generator was used to produce dry particles consisting of pure sodium chloride. These particles passed through the uncalibrated Classifier (producing a monodisperse aerosol of unknown size) before continuing on to the cloud chamber. The cloud chamber was set at one of four known supersaturations (Table 3.1). The voltage across the Classifier was then increased slowly until droplets were observed by the OPC, indicating that the critical radius (corresponding to the critical supersaturation present) had been reached. The procedure was repeated at the same four supersaturations (Table 3.1) for ammonium sulfate particles as well. The sodium chloride and ammonium sulfate tests provided a data set of eight points comparing the Classifier voltage to the critical supersaturation. Linking the critical supersaturation to the critical radius allows the calibration between the Classifier voltage and particle size to be completed.

Since the composition of the particles and the supersaturation were known, it was possible to use activation theory in reverse to calculate the radius of the dry particle. First, Equation (1.6) was rearranged to solve for b_N, giving

$$b_N = \left(\frac{2}{3\sqrt{3}} \frac{a^{3/2}}{S_c} \right)^2 \qquad (3.1)$$

where all variables are as given for Equation (1.6). The b_N term can also be given by Equation (1.5). This allowed the right-hand portions of Equations (3.1) and (1.5) to be set equal.

$$\frac{i\, m_N}{(4\pi/3)\, \rho_s\, r^3} = \left(\frac{2}{3\sqrt{3}} \frac{a^{3/2}}{S_c} \right)^2 \qquad (3.2)$$

As before, the term m_N is equal to the mass of the nucleus multiplied by the molecular weight of water and divided by the molecular weight of the nucleus material. All variables are known for Equation (3.2) except for the mass of the nucleus. Therefore, by inserting all known variables, the mass of the dry nucleus particles can be found. Based on the assumption of spherical particles and the known composition and densities of the particles, it is a simple matter to calculate the radii of the particles.

Since the activation theory was used in the calibration, agreement between the sodium chloride and ammonium sulfate data for this experiment and the data from previous observations by Twomey (1977a) is ensured. The radii that were calculated for the sodium chloride and ammonium sulfate particles at the four supersaturations are presented in Table 3.2. The Classifier voltages that correspond to these particle radii are given in Table 3.3. A regression was performed on this data set (Table 3.3) using the computer program SPSS in order to obtain an equation to convert from the Classifier voltage to the actual dry particle diameter for particles of unknown composition (note that the diameter and not the radius is desired). The relation that was obtained is

$$\text{Dry Diameter} = 0.011746*\ln(\text{voltage}) - 0.008435 \qquad (3.3)$$

The linear correlation coefficient for this fit is $R^2 = 0.94429$. This indicates a good fit between the equation and the data. A plot of Equation (3.3) along with the data from Table 3.3 is presented in Figure 3.1. This equation was used throughout the remaining experiments to link observed classifier voltage to particle size.

Table 3.2: Classifier Calibration Particle Radii

ΔT [° C]	Savg [%]	NaCl r_c [um]	$(NH_4)_2SO_4$ r_c [μ m]
3.2	0.354	0.0218	0.0267
3.5	0.423	0.0193	0.0237
3.75	0.485	0.0176	0.0216
4.0	0.550	0.0162	0.0199

Table 3.3: Particle Radius vs. Voltage for Classifier Calibration

Particle Radius [μ m]	Voltage Setting
0.0162	37
0.0176	45
0.0193	50
0.0199	50
0.0216	82
0.0218	82
0.0237	142
0.0267	170

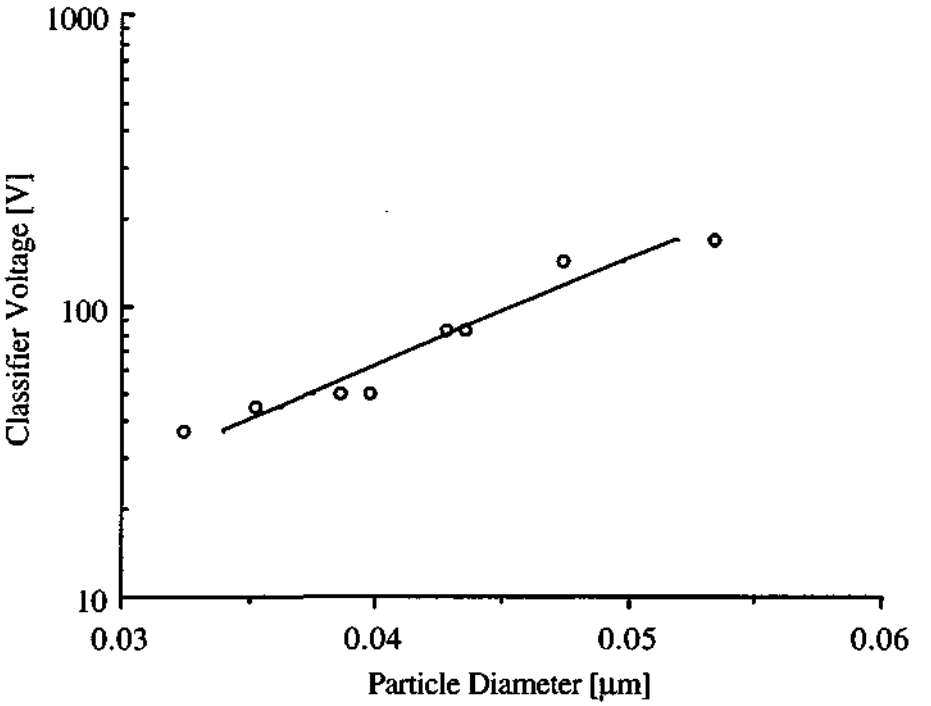

Figure 3.1: Calibration Curve: Particle Diameter vs Classifier Voltage Setting (The straight line represents the equation relating the voltage and the diameter which was developed from the data.)

3.3 Establishing Classifier Calibration

The experimental apparatus for this experiment proved to be very sensitive to any changes, whether intentional or accidental, in the air flow rates. This was especially true for the Classifier. Even slight changes in either the sheath air or sample air flow rates resulted in the Classifier selecting a particle size seemingly inconsistent with the voltage setting. Therefore, it was necessary to devise a method to verify the flow rates prior to each CCN test. This was done by passing sodium chloride particles through the CFD chamber with the plates held at a 4 ° C temperature difference. The critical size for sodium chloride particles at this supersaturation was known to correspond to a Classifier setting of 37 volts. Therefore, droplet formation at 37 volts verified proper operation. Once the

Classifier calibration was checked, the supersaturation in the CFD chamber could be adjusted to the desired value for testing.

3.4 CCN Experimental Results

All of the samples provided by UMR were collected in Rolla, Missouri. Thus, the samples all represent inland CCN. Three separate CCN samples were collected by UMR for this experiment. The first two samples, which shall be referred to as CCN-1 and CCN-2, were collected on the 8.5 by 11 inch fiberglass filters that were discussed in section 2.3.2. The third sample, CCN-3, was collected on a 47 mm quartz filter. The reason for the two different filter types is that samples CCN-1 and CCN-2 were collected during preliminary runs of the CFD chamber system. Sample CCN-3 was collected after the system was altered. Another difference between sample CCN-3 and the two earlier samples is the CCN cutoff size. The size cutoff for samples CCN-1 and CCN-2 was set to allow for the capture of all CCN particles smaller than 0.5 μm in diameter. These samples, therefore, represent "total" CCN [both large ($0.1 > d_p > 0.5$ μm) and small ($d_p < 0.1$ μm) CCN]. Sample CCN-3, however, was placed so as to collect only the coarse flow from the second impactor in the UMR system. This results in a sample of large CCN ($0.1 < d_p < 0.5$ μm) only.

For each of the filters, the sampling time was 24 hours. The total mass loadings for samples CCN-1, CCN-2, and CCN-3 were 4.6 mg, 2.7 mg, and 11.12 mg respectively. The soluble portion of each sample was extracted by the methods discussed in section 2.3.2 and then placed in the particle generator. The voltages corresponding to droplet formation at each of the four supersaturations listed in Table 3.1 were then determined. In order to ensure reproducibility of results, droplet formation for each CCN sample was examined at least twice for each supersaturation. Droplet formation was always observed at the same voltage for each individual data point, indicating the results were highly reproducible. Table 3.4 gives the observed voltages corresponding to the CFD

supersaturations settings. The dry particle diameters (critical diameters) which were calculated from these voltages using Equation (3.3) are presented in Table 3.5. Note that a "critical diameter" is simply twice the value of a "critical radius", r_c, as discussed in section 1.6.

Table 3.4: CCN Sample Classifier Voltage Settings

	Classifier Voltage Settings		
Sc [%]	CCN-1	CCN-2	CCN-3
0.354	142	170	180
0.423	130	120	130
0.485	90	100	110
0.550	50	50	60

Table 3.5: CCN Critical Diameters (Calculated from Table 3.4 values)

	Critical Diameter [μ m] *		
Sc [%]	CCN-1	CCN-2	CCN-3
0.354	0.0498	0.0519	0.0527
0.423	0.0487	0.0478	0.0487
0.485	0.0444	0.0457	0.0468
0.550	0.0375	0.0375	0.0397

* The minimum dry particle size for nucleation at a certain Sc.

3.5 Comparison With Behavior of Suspected CCN Materials

As previously discussed, ammonium sulfate and sodium chloride have long been suspected of making up the majority of the CCN material. Therefore, these were the known materials that were examined with the experimental apparatus. The data collected for ammonium sulfate and sodium chloride provided a basis for comparison for the actual CCN data which were collected. Two separate methods of comparison were used in an attempt to determine which of the two suspected materials was responsible for the activation characteristics of the CCN samples. The first method involves a graphical

comparison of the data sets. The second method, which will be presented later in this chapter, involves a numerical comparison.

3.5.1 Graphical Comparison

The data collected in this experiment were plotted in terms of dry particle radius versus the critical supersaturation required for droplet growth. A plot of this type allowed for easy comparison of the behavior of two or more materials in a supersaturated environment. Twomey (1977a) developed such a plot for sodium chloride and ammonium sulfate. A similar plot is presented in Figure 3.2. The sodium chloride and ammonium sulfate data collected for this experiment were also plotted on this graph in order to establish agreement between the two. Since the data did agree, Twomey's curves for sodium chloride and ammonium sulfate were used as the basis for the CCN behavioral comparison.

In order for the CCN data to be plotted on the same graph as the Twomey ammonium sulfate and sodium chloride curves, the x-axis of the curves had be be changed to dry particle diameter. Once this was done, the values from Table 3.5 for each individual CCN sample were plotted along with the two Twomey curves. The resulting plots for samples CCN-1, CCN-2, and CCN-3 are presented in Figure 3.3, Figure 3.4, and Figure 3.5 respectively. Figure 3.6 shows a graph consisting of all three CCN samples plotted simultaneously against the ammonium sulfate and sodium chloride curves. Note that for all of these plots, the y-axis is a linear scale as opposed to the log scale used for Figure 3.2. This was done to make the visual comparison of the data and the curves easier.

The analysis of Figures 3.3, 3.4, 3.5, and 3.6 proved relatively simple. For all of these graphs, the points representing the CCN samples fit almost exactly along the ammonium sulfate curve. Only a few of the CCN data points strayed from this curve and none coincided with the sodium chloride curve. Thus, the graphical comparison indicated that all of the CCN samples behaved as ammonium sulfate particles. This, in turn, pointed

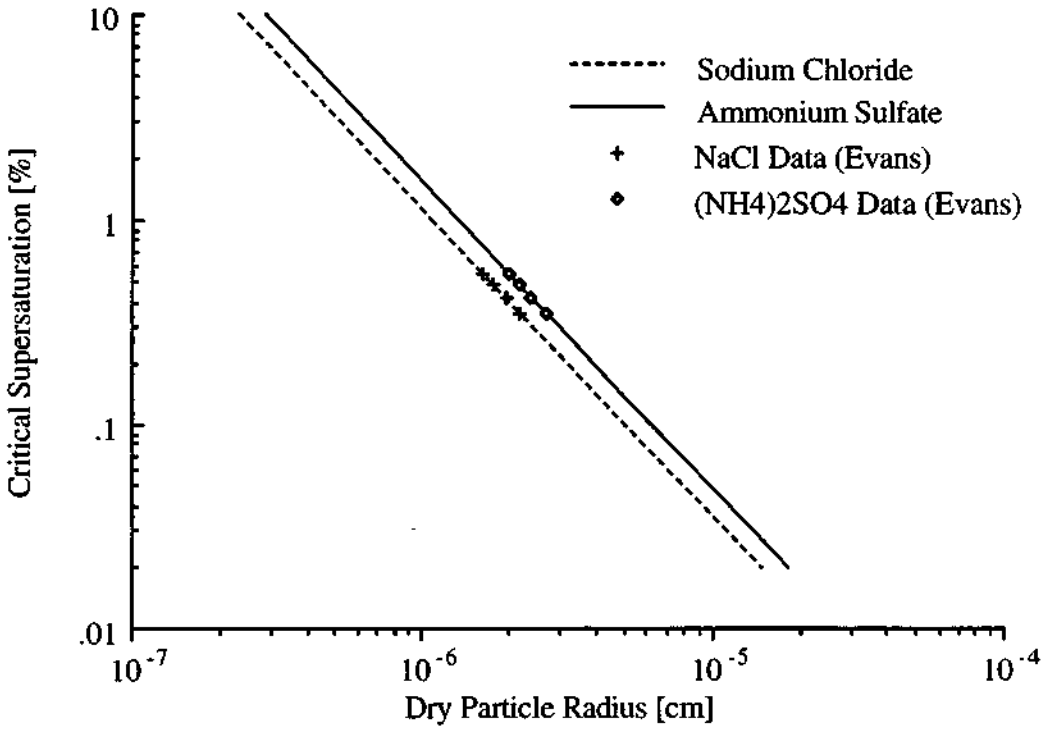

Figure 3.2: Critical Supersaturation vs Dry Particle Radius for Sodium Chloride and Ammonium Sulfate (The curves represent data collected by Twomey [1977a]. The points indicate this experiment)

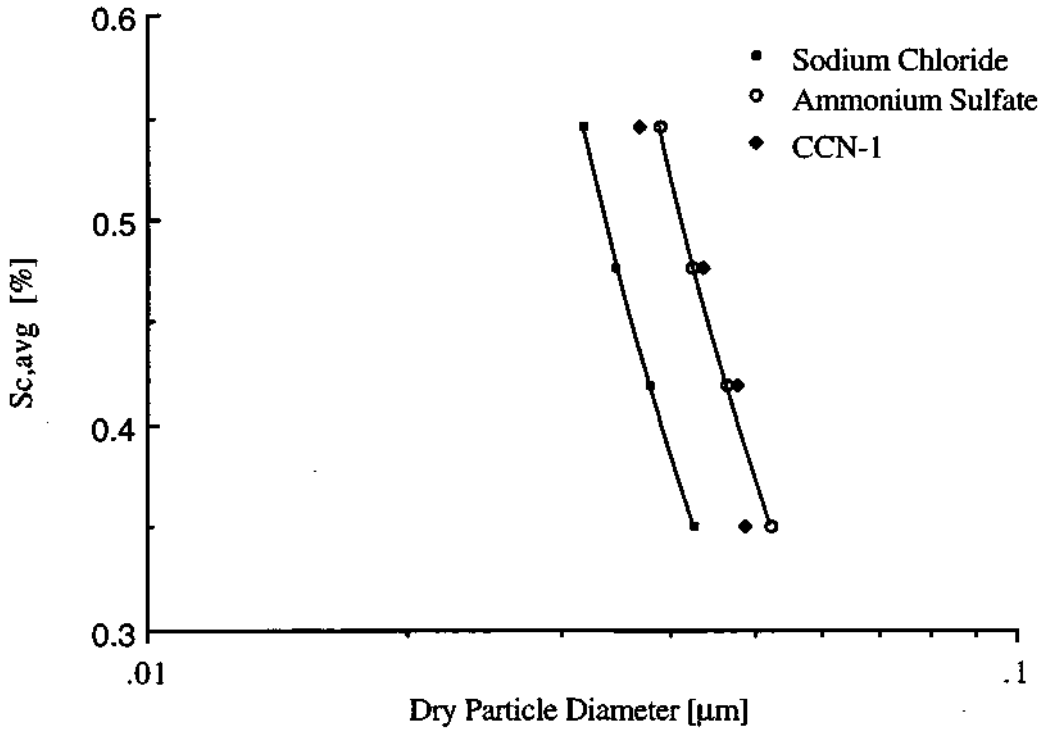

Figure 3.3: Critical Supersaturation vs Particle Diameter for CCN-1 (Comparing CCN-1 to (NH4)2SO4 and NaCl)

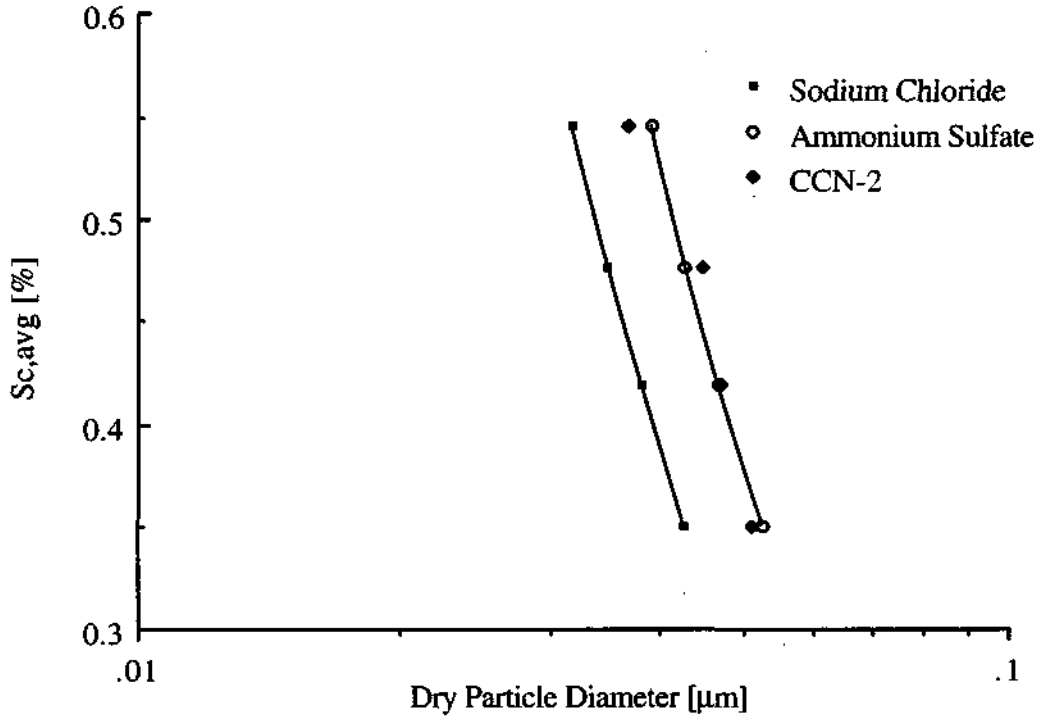

Figure 3.4: Critical Supersaturation vs Particle Diameter for CCN-2 (Comparing CCN-2 to (NH4)2SO4 and NaCl)

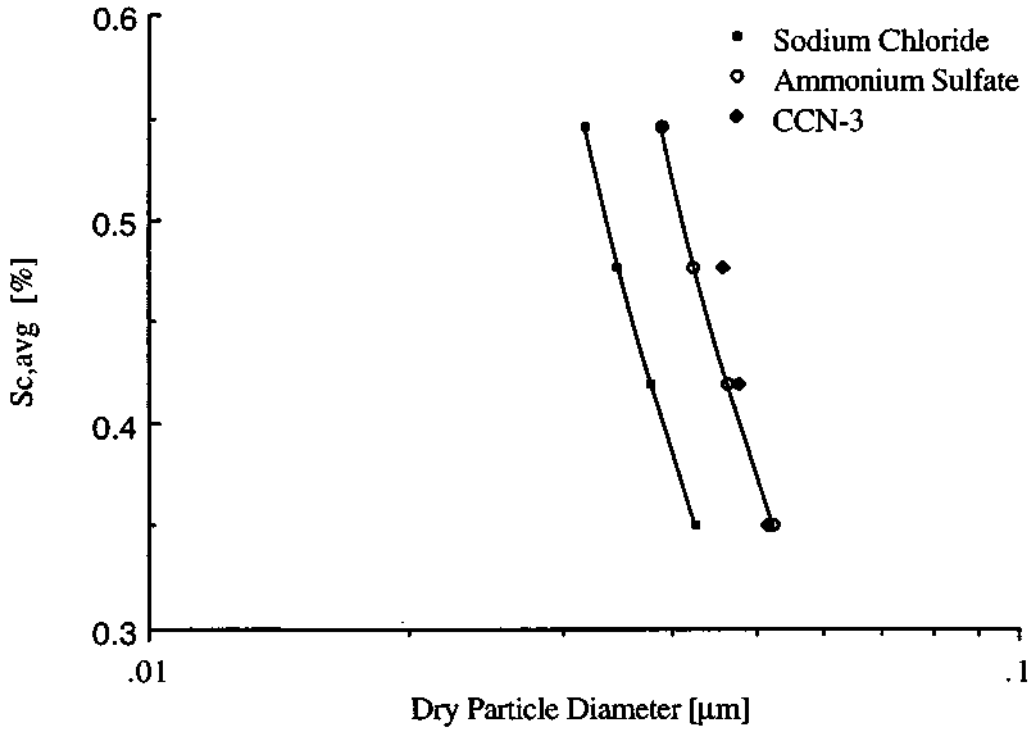

Figure 3.5: Critical Supersaturation vs Particle Diameter for CCN-3 (Comparing CCN-3 to (NH4)2SO4 and NaCl)

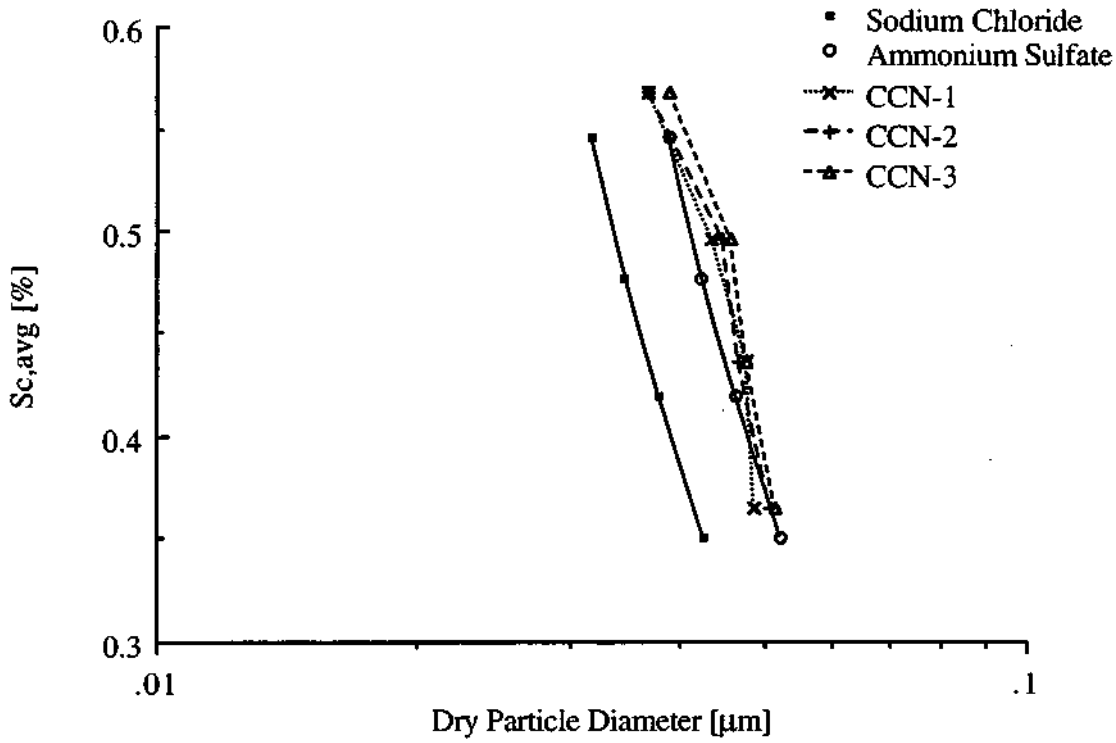

Figure 3.6: Critical Supersaturation vs Particle Diameter for All CCN (Comparing all CCN samples to (NH4)2SO4 and NaCl)

to ammonium sulfate as the component in the CCN which controls activation. Without knowledge of the actual composition of the CCN particles, however, this hypothesis was still uncertain. There still might be another substance, such as a soluble organic film, which is controlling the activation of the particles. Therefore, it was necessary to perform calculations upon which numerical comparisons of the data could be based.

3.6 Calculation of Composition Factors for CCN and Known Materials

In order to facilitate a numerical comparison between the actual CCN data sets and the known materials, it was necessary to develop a relevant factor which could readily be calculated from the available data. This factor should be dependent solely on the chemical composition of the particles if possible. This would allow for direct comparison between the CCN samples, ammonium sulfate, and sodium chloride independent of particle size. Such a term was developed by considering activation theory. First, Equation (1.6), which deals with the critical supersaturation, was rearranged to solve for b_N. This new relation is

$$b_N = \left(\frac{2}{3\sqrt{3}} \frac{a^{3/2}}{S_c}\right)^2 \qquad (3.4)$$

where all variables are as listed for Equation(1.6). The b_N term, by definition, is also equal to the relation presented in Equation (1.5).

$$b_N = \frac{i m_N}{(4\pi/3)\rho_s} \qquad (1.5)$$

The mass of the particle is equal to

$$\text{mass} = \left(\frac{4\pi}{3} r^3\right) \rho_N \qquad (3.5)$$

where ρ_N is the density of the nucleus material and r is the radius of the nucleus (particle). Plugging Equation (3.5) along with the definition of m_N given for Equation (1.5) into Equation (1.5) yields

$$b_N = \frac{i\, M_w\, r^3\, \rho_N}{M_N\, \rho_s} \qquad (3.6)$$

where all variables are as listed for Equation (1.5). It was then possible to set the right hand portions of Equations (3.4) and (3.6) equal to each other.

For each CCN sample, the critical supersaturations (S_c) and critical particle radii (r) were known from the collected data. The curvature term (a) was already known from previous calculations. Since its value varied only slightly with changing supersaturations, its value was assumed to be constant for these calculations. The molecular weight of water (M_w) as well as its density (p_s) were also already known. The values used for the curvature term (a), M_w, and p_s were 1.05 x 10^{-9} meters, 18 g/mole, and 1000 kg/m^3, respectively. This left only the van't Hoff factors (i), particle densities (ρ_N), and particle molecular weights (M_N) as unknowns. Each of these variables depended only upo?n the chemical composition of the nucleus particle. Therefore, the relation formed by equating Equations (3.4) and (3.6) was rearranged in order to separate the three variables depending only on chemical composition. This new relation is given by

$$\left(\frac{i\,\rho_N}{M_N}\right) = \Omega = \left(\frac{\rho_s}{M_w\, r^3}\right)\left(\frac{2}{3\sqrt{3}}\,\frac{a^{3/2}}{S_c}\right)^2 \qquad (3.7)$$

where all variables are as listed for Equations (1.5) and (1.6). The combination of these three variables was labelled Ω for easier discussion. The Ω term is equal to the number of ions per unit volume formed by a solution of the solid material in water.

Once Equation (3.7) was developed, calculating the Ω for the CCN samples as well as the ammonium sulfate and sodium chloride samples was a simple matter. First, however, a check of the accuracy of the relation was performed. The ammonium sulfate and sodium chloride samples proved ideal for this purpose since not only were critical supersaturation versus critical radius data available, but the exact chemical composition was known as well. Thus, P_N, M_N, and i were already known. These values which were used

for these calculations are presented in Table 3.6. This allowed for the calculation of the expected Ω values for the two materials. The Ω values were then also calculated by plugging the data for all four supersaturation settings presented in Table 3.2 into Equation (3.7). These values, along with the expected values and the deviation from these values, are presented in Table 3.7.

Table 3.6: Values of ρ_N, M_N, and i for Sodium Chloride & Ammonium Sulfate

Variable	Units	$(NH_4)_2[SO]$	NaCl
PN	g/cm^3	1.769	2.165
M_N	g/mole	132	58.4
i		3	2

Table 3.7: Ω Values Calculated for $(NH4)_2SO_4$ and NaCl

	Calculated from the Data	
Sc [%]	Sodium Chloride Ω rions/unit voll	Ammonium Sulfate Ω rions/unit voll
0.354	74,064.5	40,081.3
0.423	74,065.1	40,097.3
0.485	74,062.3	40,082.2
0.550	74.044.8	40.121.0
Mean Ω	74,059.2	40,095.5
std. dev.	8.4	16.1
Expected Ω	74,093.1	40,204.4
% Error	0.05 %	0.27 %

A comparison of the experimental and expected values from Table 3.7 showed excellent agreement between the two. Therefore, the Ω values for the three CCN samples were also calculated at each supersaturation. These values are presented in Table 3.8 along with their mean values. The standard deviations for the calculated means of each of the CCN samples were around 10 %. A statistical analysis was performed on the Ω values of the CCN samples using the Student-T test for comparing two mean values. This test

indicated that the Ω values for all three CCN samples are statistically equal at a confidence level of 95%.

Table 3.8: Ω Values Calculated for CCN Samples

Sc [%]	CCN-1 Ω	CCN-2 Ω	CCN-3 Ω
0.354	49,421.2	43,634.2	41,986.7
0.423	36,903.6	39,123.8	36,903.6
0.485	37,074.7	34,135.5	31,741.9
0.550	47.636.4	47.636.4	40.333.8
MeanQ	42,759.0	41,132.5	37,741.5
std. dev.	5.804.5	5.038.7	3.919.2

3.6.1 Comparison of CCN Sample and Known Material Ω Values

Once the Ω's were calculated for the three CCN samples, it was possible to compare their mean values to those of ammonium sulfate and sodium chloride. The percent difference between the mean values for the three CCN samples and the expected Ω's for the two known materials are presented in Table 3.9. These values show that the Ω*'s* for all three CCN samples did not agree with the Ω expected for sodium chloride but did agree with the expected Ω for ammonium sulfate. In order to provide statistical proof of this observation, another Student-T test was performed on the Ω value data. The test was used to compare the Ω values of the CCN samples to the Ω values for ammonium sulfate and sodium chloride. This analysis showed that the Ω values for all three CCN samples are statistically equal to the Ω value for ammonium sulfate at a confidence level of 95 %. The test also found that the Ω values for the CCN samples are statistically different from the Ω value for sodium chloride at a confidence level of 95 %. Thus, this method indicated ammonium sulfate, not sodium chloride, was controlling the behavior of the CCN particles.

The results of the statistical analysis of the Ω values, along with the graphical comparison, clearly pointed to ammonium sulfate as the soluble component of CCN that

was controlling the activation characteristics of the CCN particles. The results did not, however, prove that ammonium sulfate was the only material present in the CCN particles. Still other material, either soluble or insoluble, might have been present in the original CCN samples. Without further tests, these components of CCN would have remained unidentified by this experiment. This limitation did not occur, however, since several chemical analyses were performed at the ISWS on the CCN samples as a part of Dr. Williams' research. The results of these tests were made available to enable further interpretation of the data collected by this experiment. A brief description of the methods used for these analyses is presented in the next section.

Table 3.9: CCN Sample Ω's Compared to NaCl and $(NH_4)_2SO_4$ Ω's

Sample	Mean Ω	NaCl % Difference	$(NH4)_2SO_4$ % Difference
CCN-1	42,759.0	42.3	5.9
CCN-2	41,132.5	44.5	2.6
CCN-3	37.741.5	49.1	5.9

3.7 Chemical Analyses of CCN Samples

The chemical composition of the CCN samples for this experiment, as well as of many other samples which were collected by UMR, were examined using several different methods. The methods used varied slightly for different filter types. Since samples CCN-1 and CCN-2 were both collected on the 8.5 by 11 inch fiberglass filters, similar methods were used for analysis of CCN-1 and CCN-2. Sample CCN-3 was collected on a 47 mm quartz filter. This required a slightly different method of analysis which will be discussed later.

For samples CCN-1 and CCN-2, the first step in the analysis was to weigh the filters to determine their loading. The soluble fractions of the samples were then extracted using the method described in section 2.3.2. The filters were then dried and weighed again to determine the amount of sample remaining on the filters. These measurements found

that the average percentage of total mass which was water insoluble for these filters was 24.4 %. After each sample was extracted from its filter, portions of the extracted sample solution were examined using various methods. For samples CCN-1 and CCN-2 (total CCN samples), the first analysis which was performed was an Inductively Coupled Plasma (ICP) analysis. This method detects the presence of 32 different elements (not including carbon). Of these 32 elements, only sulfur was detected in significant quantities (after correction for readings of blank filters). Both sodium and chlorine were below the detection limits of the instrument, indicating that sodium chloride is not present in great quantities in the CCN collected by these samples. Portions of the filter samples were then analyzed by Ion Chromatography (IC). This method detected only sulfate (SO_4^{2-}) and ammonium (NH_4^+) ions in significant quantities. The average reading for sulfate was 37.9 % by mass, assuming the sulfate is present as ammonium sulfate. The average value for ammonium was 37% by mass, again assuming it is present as ammonium sulfate. The close agreement between the two values and the relative absence of any other non-organic ions makes this a valid assumption. Also, the mass of sulfur detected by the ICP analysis, when converted to ammonium sulfate mass, differs from the IC value by only 12 %. A similar examination was performed on samples collected on 47 mm teflon filters using X-Ray flourescence (XRF). This analysis found the sample consisted of 9.1 % sulfur, which corresponds to 37.5 % of the total mass if the sulfur is present as ammonium sulfate. This also corroborates the amount indicated by the IC analysis. Since these measurements indicated that 37.9 % of the mass was ammonium sulfate and only 24.4 % of the total mass was insoluble, 37.7 % of the CCN mass was unaccounted for. This portion of the CCN material must have been a water soluble substance which was not ammonium sulfate. Since the methods used for the analyses of the samples collected on the fiberglass filters were unable to identify this unknown material, further tests were required.

It was postulated that this remaining material might be organic (i.e., containing carbon linked with hydrogen and other elements). The large fiberglass filters were not

suitable for analysis for carbon content, so new CCN samples were collected on 47 mm Whatman quartz fiber filters. The quartz filters were well suited for these tests since quartz has a high affinity for organic materials and a low carbon blank. Also, it was possible to pre-fire the filters at high temperatures in order to drive off any organics which might have been present on the filter prior to CCN sampling. Sample CCN-3 consisted of large CCN collected on this type of filter. Nine other CCN samples were also collected in this manner. These filters were each divided into three sections. The first section was analyzed by IC in order to determine their ammonium sulfate content. The second section of each filter was immediately analyzed for total carbon using a thermo-optical system. This method involved heating the sample to 850 ° C in a high oxygen atmosphere in order to convert the carbon to carbon dioxide. The amount of CO_2 formed was then analyzed by non-dispersive infrared detection. Thus, the total amount of carbon present in the sample was determined. Finally, the third section of each filter was rinsed with five solvents in series in order to remove any soluble organic compounds. These solvents, in order, were water, a 50 % hexane/acetone mixture, dichloromethane, ethyl ether, and methanol. After this extraction was completed, the filter sections were allowed to dry. These dry sections were then analyzed using the thermo-optical system in order to measure the amount of insoluble carbon that was present on the filters. This insoluble carbon was interpreted to be elemental carbon (i.e., soot). By subtracting the insoluble (elemental) carbon fraction from the total (elemental and organic) carbon on the filters, the soluble carbon fraction, which corresponded to the organic carbon fraction, was determined for each sample.

The measured soluble carbon gave the mass of only the carbon that was present in the organic compounds in the sample. Obviously, carbon was not the only atom present in these molecules. Therefore, it was necessary to somehow relate the organic carbon mass to the mass of organic compounds present in the original sample. Jaenicke (1978) calculated that the approximate carbon compound mass could be found by multiplying the measured carbon mass by 1.41. This use of this multiplier, however, gave total theoretical masses

which were 90% of the measured values. Missing such a large amount of material during analysis seemed unlikely. By multiplying the carbon mass by a factor of 2, however, gave total theoretical masses which were 99.5 % of the measured sample masses. Therefore, to uphold conservation of mass, this multiplier was used.

These above methods resulted in the development of a data set that contained the total mass (by weighing the filters before and after sampling), and the masses of ammonium sulfate (from IC analysis), organic carbon, and elemental carbon in the CCN samples. By performing a multiple linear regression comparing these three masses to the total mass, the average percentage of each was calculated. For these regressions, each component mass measured for the nine filter samples was individually compared to the total mass on the filters for these samples. The correlation coefficients for these three regressions were all above 0.90, indicating a good fit. The average organic compound mass was then calculated from the average organic carbon mass (16.1 %) using the factor of 2 multiplier. Table 3.10 presents the measured percentages of the three components of the CCN samples along with their corresponding correlation coefficient, R^2. These values should also apply to sample CCN-3 since it was collected during the same sampling period as the other nine samples.

Table 3.10: Large CCN Composition

Material	% of Total Mass	Correlation
$(NH4)_2SO_4$	63.3	0.996
Organic Compound	32.2	0.925
Elemental Carbon	4.0	0.906

A considerable difference was observed between the percentages found on the quartz filters (Table 3.10) and those measured for the samples collected on the 8.5 by 11 inch fiberglass filters. The average ammonium sulfate amount detected on the fiberglass filters was smaller than that for the quartz filters. Conversely, the non-ammonium sulfate

soluble material, which could be interpreted as organic material, was present in larger amounts on the fiberglass filters than the quartz filters. This difference occurred because the samples collected on the fiberglass filters were for total CCN while the samples on the quartz filters were for large CCN only. Analyses of small CCN samples collected on quartz filters showed that the small CCN contained smaller percentages of ammonium sulfate and greater percentages of organics than did the large CCN. Therefore, the presence of the small CCN in the total CCN samples brought down the average ammonium sulfate percentages while increasing the overall organic compound percentages. The small CCN composition values were not included here since critical supersaturation data were only collected for large and total CCN samples.

3.8 Numerical Analysis of Organics Present in CCN

The chemical analyses performed on the CCN samples showed that organic compounds are indeed a major component of CCN. The methods used were unable, however, to identify which organic compounds were present in the samples or to determine their activation characteristics. Without an understanding of the composition or behavior of this component of CCN, it would have been impossible to rule out that the organics were actually controlling the activation of the particles used for this experiment. Therefore, further analysis of the organic component of the CCN was performed using the data presented in Table 3.10 as well as the Ω values which were calculated for ammonium sulfate and the CCN.

3.8.1 Calculation of Ω for the Organic Component of CCN

The goal of these calculations was to determine the Ω of the organic compounds present in the CCN samples. Since Ω depends solely on particle composition, determining the Ω for the organic compounds was an ideal way to compare the organics to the CCN samples as well as the known materials. For these calculations, only the data set for

sample CCN-3 (a large CCN sample) was used since this was the only sample for which the organic fraction of the sample could be estimated. Therefore, all calculations which were performed related to large CCN.

The method which was used to calculate the Ω for the organic compounds was a simple mass balance. For this mass balance, it was necessary to determine exactly what portion of the CCN was soluble organic compounds. The chemical analyses which were performed on the samples found that 40.9 % of the organic carbon compound was water soluble. Since only the soluble portion of the CCN was activated, this was the portion of the organics which was of interest. The fraction of total CCN mass which was water soluble organic compounds was obtained by multiplying the organic fraction of CCN mass (32.2 %) by the fraction of organics that were soluble (40.9 %), yielding

$$\text{Soluble Organics Fraction} = (0.322)(0.409) = 0.1317 = 13.17\ \%.$$

The other soluble portion of the CCN samples was the ammonium sulfate. It was assumed that 100 % of the ammonium sulfate was soluble. According to the analysis presented in Table 3.10, 63.3 % of the total CCN sample was ammonium sulfate. Since the elemental carbon fraction was insoluble it did not enter into this calculation.

Once the fractions for the total CCN were calculated, it was necessary to calculate the fractions of soluble organics and ammonium sulfate present in the soluble CCN sample. Since the insoluble elemental carbon fraction was not present in the soluble CCN sample, the percentages of ammonium sulfate and the organic compounds as compared to the total soluble mass were greater than for the total CCN samples. These values were required since only the soluble portion of the CCN was examined by this experiment. The ammonium sulfate fraction in the soluble CCN sample was calculated by dividing the percentage of ammonium sulfate in the total sample (63.3 %) by the sum of the ammonium sulfate (63.3 %) and organic compounds (13.17 %) present in the total CCN sample This gave a value of 82.78 % for the ammonium sulfate fraction of the soluble CCN. A similar

calculation for the organic compounds gave a value of 17.22 % for the fraction of soluble organics present in the soluble CCN sample. Note that these values add up to 100 %. Therefore, the mass balance (assuming that only ammonium sulfate and organic compounds were present) for the Ω values was

$$0.8278\ \text{Qamsul} + 0.1722\ \Omega_{\text{organics}} = \Omega_{CCN-3} \qquad (3.8)$$

where Ω_{amsul} is for ammonium sulfate.

Since the Ω's for ammonium sulfate and sample CCN-3 had already been calculated, the Ω for the organics was the only remaining variable. The ammonium sulfate and sample CCN-3 values were 40,095.5 and 37,741.5 respectively. This resulted in an Ω for the organic compounds of

$$\Omega_{organics} = 26{,}425.3$$

This number was considerably smaller than the values for sample CCN-3 as well as ammonium sulfate. Since the activation of a particle depends heavily upon its Ω value, the possibility that the organics were controlling the activation of the large CCN particles was ruled out. Therefore, it was determined that ammonium sulfate was indeed the component which controlled the activation characteristics of the large CCN. The same could not be said with any confidence, however, for small CCN since no critical supersaturation data were available for the small size fraction. Despite the fact that the activation of the CCN particles was not dependent upon the organic compounds, the behavior of the organics in supersaturated conditions was still of interest. Thus, further calculations to determine their activation characteristics were performed.

3.8.2 Calculation of the S_c for the Organic Compounds

Once the Ω of the soluble portion of the organic compounds in the CCN was determined, it was possible to calculate the critical supersaturation of particles consisting solely of this material. This was done to determine whether the presence of the organics

inhibited, promoted, or had no effect upon the activation characteristics of the CCN particles. These calculations were performed by first assuming a dry particle size for a particle consisting entirely of the organic compounds. It was then possible to calculate the b_N corresponding to this size using Ωorganics and Equation (3.6). Once b_N was determined, it was possible to calculate the critical supersaturation using Equation (1.6). Once again, the value of the curvature term (a) was assumed constant for these calculations. This procedure was performed at numerous dry particle diameters. The critical supersaturations required by similarly sized particles consisting entirely of ammonium sulfate and sodium chloride were also calculated using this method. The results for all three materials are presented in Table 3.11.

Table 3.11: Critical Supersaturations Required for Various Particle Materials

Dry D_p [μ m]	NaCl Sc [%]	$(NH_4)_2SO_4$ Sc [%]	Organics Sc [%]
0.(53	0.618	0.838	1.034
0.04	0.402	0.544	0.671
0.05	0.287	0.389	0.480
0.06	0.219	0.296	0.365
0.07	0.173	0.235	0.290
0.08	0.142	0.192	0.237
0.09	0.119	0.161	0.199
0.10	0.102	0.138	0.170
0.20	0.036	0.049	0.060
0.30	0.020	0.027	0.033

A comparison of these critical supersaturations shows that a particle consisting entirely of the organic compounds would require a greater supersaturation for activation than both sodium chloride and ammonium sulfate. Therefore, the presence of the organic compounds in the large CCN most likely slightly retard the activation of the particles tested. The S_c values calculated for the organic compounds were not, however, so great as to completely prevent the activation of a particle consisting solely of this material under natural conditions. Thus, it would appear that the activation of the CCN particles could have been

controlled by the organic compounds if the organics had composed a greater fraction of the CCN material.

3.9 Conclusions

The data sets which were collected for this experiment were interpreted in several different ways. Each method indicated that ammonium sulfate was the component of the soluble fraction of the large CCN as well as of the total CCN samples which controlled the activation characteristics of the particles. This result agrees well with earlier studies as well as the indirect evidence which points to ammonium sulfate active CCN particles. Sodium chloride, on the other hand, did not appear to have any significant effect on droplet formation for the samples tested. This was not surprising since the chemical analysis of the CCN samples indicated that only insignificant amounts of sodium chloride were present.

The data collected for this experiment were also used to calculate the composition factor, Ω, for the organic compound portion of the CCN. This value was determined to be 26,425.3, which was considerably lower than the ammonium sulfate, sodium chloride, and CCN sample values. Thus, it was determined that the organic compounds were not controlling the activation characteristics of the CCN. Further calculations, based on the value of $\Omega_{organics,}$ determined that the organic materials present in the CCN required slightly higher supersaturations than ammonium sulfate particles. Therefore, the presence of the organic materials appeared to have a retarding effect on the activation of the large CCN particles. It was not possible to say whether the organics were present purely as a surfactant or if they were intermixed throughout the particle. It would appear that if the organic compounds had entirely coated the particle surfaces, that the CCN particles would have required a higher supersaturation for activation to occur. Such a determination could not be made since the method of reproducing the CCN particles most likely altered their internal arrangement.

Although the critical supersaturations required for the activation of particles entirely composed of the organic compounds were greater than for corresponding particles of ammonium sulfate, they were not so large as to prevent activation under natural conditions. Such particles could activate even at sizes as small as 0.03 μm in diameter. Thus, these particles would satisfy Twomey's (1977a) calculated mean upper size limit of 0.06 μm in diameter for CCN particles. These results indicated that the organic material or materials present in the CCN samples have a high activity. This fact, coupled with the greater fraction of organic compounds and lesser fraction of ammonium sulfate found in the small CCN samples as compared to the large CCN samples, could result in the activation characteristics of the small CCN being controlled by the organics. This determination could not be made, however, since no data were collected for small CCN.

3.10 References

Jaenicke, R., "The Role of Organic Material in Atmospheric Aerosols," *Pure Appl. Geophys.* **116,** 283-292, 1978.

Twomey, S., Atmospheric Aerosols. Elsevier Scientific Publishing Company, Amsterdam, 1977 a.

Chapter 4

Recommendations for Future Work

4.1 Overview

Several aspects of the behavior as well as the composition of cloud condensation nuclei have been determined by this research. Ammonium sulfate was determined to be the dominant component of both large CCN and the overall CCN for the samples studied. Also, the composition factor, £2, and critical supersaturation requirements for the organic compounds present in the CCN samples were calculated. However, questions were left unanswered due to the lack of data. Therefore, further research is required in these areas.

4.2 Recommendations

In order to gain a more complete understanding of the behavior and composition of CCN, the following work should be performed. First, data should be collected on the critical supersaturations for the soluble fraction of small CCN samples using this apparatus or one similar to it. Such samples could be used to determine, both graphically and numerically, which component of the small CCN is controlling the activation of the particles in the atmosphere. If this data should indicate that the organic compounds are controlling the activation of the particles, further tests could be performed in an attempt to determine which organic compound or compounds are actually present. This could possibly be done by activating known organic compounds in a cloud chamber system such as the one used for this experiment in order to obtain critical supersaturation data for these compounds. This data could then be compared to the data for the small CCN samples. Also, additional direct chemical composition tests should be performed on both the small and the large CCN. The samples tested should also include ones collected in or near a marine environment in order to determine the effects of the presence of sodium chloride in the CCN.

In addition to performing additional analyses using the present system, attempts could be made to improve the methods used to collect the critical supersaturation data. The present system requires the capture and resuspension of the CCN particles in order to test them. This most likely alters the overall composition and arrangement of the particles somewhat. A better way to test these particles would be to pass the droplets formed on the CCN in the large cloud chamber system through a dryer and then directly to the smaller cloud chamber system. This would allow for the examination of the insoluble fraction of the CCN. Also, any errors which might be present in the data collected for the soluble fraction of the CCN would be reduced. There would also be less disturbance of the arrangement of the components of the CCN particles since far less mixing would occur. Thus, data could be collected on the way that actual CCN particles behave in the atmosphere. It should be noted that much of this work will be performed in the future as part of the research being performed by the ISWS and UMR.

Appendix A

Computer Program for Cloud Chamber and OPC Control

Appendix A

Computer Program for Cloud Chamber and OPC Control

The following program was written to control of the cloud chamber supersaturation and collect the data from the OPC. The system used one external access board (EXP-GP) and an additional internal analog input board (DAS-8PGA) to enable the computer to read the thermistors and control the heaters. The EXP-GP board output channel should be connected to Channel #0 on the DAS-8PGA board for proper operation. The program was written in the Quick Basic language on an IBM 386 personal computer.

The Program:

```
'  Initialization for the temperature control portion
10  DIM D%(7), CH%(7), YL%(7)    '8 elements, one for each EXP-GP channel
'  Also initialize a corresponding real array to receive temperature data
DIM T(7)
DIM LT%(7)
COMMON SHARED D%(), LT%()
DECLARE SUB DAS8 (mode%, BYVAL dummy%, FLAG%)
DIM ATEMP AS STRING * 580
CLEAR, 49152!
zx% = 0:  zy% = 0:  zz% = 0
'  Setup for OPC data taking
status = 0   '0 = on
ON COM(l)  GOSUB SAMPLE
'
OUT &H343, &H80    ' Initialize the DAS8-PGA
OUT &H341, &H1      ' Open valve to purge pms tube while not sampling
'  This portion of the program interfaces with the PMS OPC
30  DEFSTR A, X
40   SCREEN 0,0,0
50  KEY OFF:  CLS:  CLOSE
60  DEFINT  I-N
70  FALSE = 0:  TRUE = NOT FALSE
80  ABLANK = STRING$(80, CHR$(32))
90  XOFF = CHR$(19):  XON = CHR$(17)
100  aline = CHR$(179)
110  ATIME = TIMES
120  ATIME = MID$(ATME, 1, 2) + MID$(ATIME, 4, 2) + MID$(ATIME, 7, 2)
130  OPEN "COM1: 9600,E,7,, CS,DS,CO" FOR RANDOM AS #1 LEN = 1024
131  REM HIST = FALSE    'Default is no histogram
133  REM PRINT "Do you want a HISTOGRAM instead of printed data?  (Y/N)  >";
135  REM ANS = INKEY$:  IF ANS = "" THEN 135
137  REM IF ANS = "Y" OR ANS = "y" THEN HIST = TRUE
```

```
140  PRINT #1,  XON:  PRINT #1, "SB Y":  PRINT #1, "ES":  PRINT #1, "MN 6":
        PRINT #1, "TD  " + ATIME
150  IF EOF(1) THEN 220
160  IF LOC(l) > 128 THEN PAUSE = TRUE:  PRINT #1, XOFF
170  ATEMP = INPUT$(LOC(l),#l)
180  IF LOC(l) > 0 THEN GOTO 170
190  IF PAUSE THEN PAUSE = FALSE:  PRINT #1, XON:  GOTO 150
220  C16 = FALSE;  GOTO 250
240  GOTO 220
250  IF C16 = TRUE THEN OPEN "defl6.dat" FOR INPUT AS #2
260  IF C16 = FALSE THEN OPEN "def32.dat" FOR INPUT AS #2
270  INPUT #2, ACONT
280  INPUT #2, AINTER
290  IF C16 = TRUE THEN INPUT #2, ARANGE
300  CLOSE #2
310  GOSUB 990
320  LOCATE 4, 1:  PRINT ABLANK
330  LOCATE 4, 22:  PRINT aline + "The Default Values Are ":  LOCATE 4,50:
        PRINT aline
340  LOCATE 11, 20:  PRINT "Do you wish to use the Default Values (Y/N)?  ";
350  ANS = INKEY$;  IF ANS = "" THEN 350
360  IF ANS = "Y" OR ANS = "y" THEN 590
370  LOCATE 11, 1;  PRINT ABLANK;
380  LOCATE 11, 20D;  PRINT "Choose continuous (C) or single (S) sampling  >";
390  ANS = INKEY$:  IF ANS = "" THEN 390
400  IF ANS = "S" OR ANS = "s" THEN ACONT = "SB Y" ELSE IF ANS = "C" OR
        ANS = "c" THEN ACONT = "SB N" ELSE 380
410  LOCATE 11, 1:  PRINT ABLANK
420 LOCATE 11, 20:  INPUT "Enter the sampling interval in seconds  >", IINTER
430  IF IINTER > 6553 OR IINTER < 1 THEN GOTO 420 ELSE AINTER =
        LTRIM$(RTRIM$(STR$(IINTER)))
440  IF C16 = FALSE THEN 490
450  LOCATE 11, 1:  PRINT ABLANK;
451  LOCATE 14, 2:  PRINT CHR$(218) + STRING$(77, CHR$(196)) + CHR$(191)
452  LOCATE 15, 2:  PRINT aline;  "Press 0 for fixed range F0  "; aline; "Press 4 for
        autorange (A2) between F0 and Fl ":  LOCATE 15, 80:  PRINT aline
453  LOCATE 16, 2:  PRINT aline;  "Press 1 for fixed range F1";  aline;  "Press 5 for
        autorange (A4) between F0 and F3":  LOCATE 16, 80:  PRINT aline
454  LOCATE 17, 2:  PRINT aline; "Press 2 for fixed range F2 "; aline:  LOCATE 17, 80:
        PRINT aline
455  LOCATE 18, 2:  PRINT aline;  "Press 3 for fixed range F3 ";  aline:
        LOCATE 18, 80:  PRINT aline
456  LOCATE 19, 2:  PRINT CHR$(192) + STRING$(77, CHR$(196)) + CHR$(217)
460  LOCATE 11, 20:  PRINT "Choose (0-5) >";
470  ANS = INKEY$:  IF ANS = "" THEN GOTO 470
480  IF ANS >= "0" AND ANS <= "3" THEN ARANGE = "F" + ANS ELSE IF
        ANS = "4" THEN ARANGE = "A2" ELSE IF ANS = "5" THEN
        ARANGE = "A4" ELSE GOTO 460
490  GOSUB 990
500 LOCATE 11,1:  PRINT ABLANK
510  LOCATE 11, 20:  PRINT "Save the current setting as the default (Y/N)?";
520  ANS = INKEY$;  IF ANS = "" THEN 520
530  IF ANS o "Y" AND ANS <> "y" THEN 590
```

```
535  IF C16 = TRUE THEN OPEN "defl6.dat"  FOR OUTPUT AS #2
540  IF C16 = FALSE THEN OPEN "def32.dat" FOR OUTPUT AS #2
550  PRINT #2, ACONT
560  PRINT #2, AINTER
570  IF C16 = TURE THEN PRINT #2, ARANGE
580  CLOSE #2
590  LOCATE 11,1:  PRINT ABLANK
600  LOCATE 11,20:  INPUT "Enter the output filename >",  AFNAME
610  AFNAME = "c:\das8V + AFNAME
620  OPEN AFNAME FOR OUTPUT AS #2
630  LOCATE 11, 1:  PRINT ABLANK
640  LOCATE 19,20:  INPUT "Enter any comments about this data set >", ACOMMENT
650  PRINT #2, ACOMMENT:  PRINT #2, " "
660  PRINT #1, ACONT:  PRINT #1, "SI" + AINTER:  IF C16 = TRUE THEN
         PRINT #1, "RA " + ARANGE
670  CLS:  LOCATE 1, 1;  PRINT "Press any key to start sampling >";
680 ANS = INKEY$:  IF ANS = "" THEN 680
690  IF ACONT = "SB N"  THEN LOCATE 1,1:  PRINT ABLANK:  LOCATE 1, 1:
         PRINT "Continuous sampling.  Press any key to stop sampling."
700 IF ACONT = "SB Y" THEN LOCATE 1,1: PRINT ABLANK: LOCATE 1,1:
         PRINT "Single sampling.  Press any key to continue."
'
PRINT #1, "SS"
701  GOTO TEMPERATURE    Temperature control for cloud chamber
'
SAMPLE:
'  Subroutine for Sampling
THav$ = STR$(T(1)):  TCav$ = STR$(T(0)  'Calculate average plate temperatures over
         each sampling interval
PLATES = "HOT = " + THav$ + "COLD = " + TCav$
zx% = zy%   'Logic for arranging data from the OPC
zy% = LOC(l)
IF zx% = zy% then zz% = zz% + 1
IF LOC(l) <290 THEN RETURN
IF zz% < 12 THEN RETURN
VIEW PRINT 9 TO 25    Location for printing OPC data on screen
zyy% = zy%
zx% = 0:  zy% = 0:  zz% = 0
CLS 2
PRINT #1, XOFF
707  FIRST = TRUE
710  PAUSE = FALSE
725  REM IF HIST = TRUE THEN PRINT # 1,  "PP"
ATEMP = INPUT$(LOC(l), #1)
zy2% = LOC(l)
770  lfp = 0;  ifp = 0
780  ifp = INSTR(lfp + 1, ATEMP, CHR$(3))
790  IF ifp > lfp THEN MID$(ATEMP, ifp, 1) = " ":  lfp = ifp:  jfp = ifp
800  lfp = 0;  ifp = 0
810  ifp = INSTR(lfp + 1, ATEMP, CHR$(3))
820  IF ifp > lfp THEN MID$(ATEMP, ifp, 1) = " ":  lfp = ifp:  GOTO 810
ATEMP1 = MID$(ATEMP, jfp, 289 )
ATEMP1 = PLATES + ATEMP1
```

```
830  PRINT#2,ATEMP1;
840  PRINT ATEMP1;
850  IF PAUSE THEN PAUSE = FALSE:  PRINT #1, XON
860  PRINT #1, XON
870 RETURN
'
875  IF ACONT = "SB Y" AND FIRST = TRUE THEN FIRST = FALSE:  GOTO 710
880  PRINT : PRINT : PRINT : PRINT "Sampling ended, file saved."
890  PRINT : PRINT : PRINT "Press any key to continue"
900  CLOSE (2)
910  ANS = INKEY$:  IF ANS = "" THEN 910
920  GOSUB 990
930  LOCATE 22, 20;  PRINT "Do you wish to continue sampling (C) or exit to
         BASIC (X) >";
940  ANS = INKEY$;  IF ANS = "" THEN 940
950  IF ANS = "C OR ANS = "c" THEN 250
960  IF ANS = "X" OR ANS = "x" THEN 980
970  GOTO 930
980  END
990  CLS
1000  LOCATE  1, 22:  PRINT CHR$(218) + STRING$(27, CHR$(196)) + CHR$(191)
1010  LOCATE 2, 22:  PRIINT aline + "  PMS INTERFACE PROGRAM":
         LOCATE 2, 50;  PRINT aline
1020  LOCATE 3, 22:  PRINT aline + "                                        ":
         LOCATE 3, 50:  PRINT aline
1030  LOCATE 4, 22;  PRINT aline + "  The Current Values Are":  LOCATE 4, 50:
         PRINT aline
1040  LOCATE 5, 22:  PRINT aline + "                                  " :LOCATE 5, 50:
         PRINT aline
1050  LOCATE 6, 22
1060  IF ACONT = "SB N" THEN PRINT aline + "1.  Continuous sampling " ELSE
         PRINT aline + "  1.  Single sampling"
1070  LOCATE 6, 50:  PRINT aline
1080  LOCATE 7, 22:  PRINT aline + " 2.  Sample interval = ";
1090  PRINT USING "\ \";  AINTER;  :  LOCATE 7, 50;  PRINT aline
1100  IF C16 = TRUE THEN LOCATE 8, 22:  PRINT aline:  LOCATE 8, 50:
         PRINT aline
1120  LOCATE 9, 22;  PRINT CHR$(192) + STRING$(27, CHR$(196)) + CHR$ (217)
1130  RETURN
'
TEMPERATURE:
'  Subroutine for input of the cloud chamber plate temperatures
INPUT ; "Desired cold plate temperature = "; ct
PRINT "
INPUT ; "Desired hot plate temperature = "; ht
PRINT "
VIEW PRINT 1 TO 9
ANS = INKEY$
PRINT #1, XON
SCREEN 0,0,0:  KEY OFF:  CLS:  WIDTH 80
GOSUB 3000:  CLS
'
PRINT #1, XON
```

```
LOCATE 25, 1:  COLORO, 7;  PRINT "-Please Wait-";: COLOR 7, 0;  PRINT
        " Loading DAS8 I/O address.":  LOCATE 1, 1
PRINT  #l,XON
OPEN "DAS8.ADR" FOR INPUT AS #3
INPUT #3, BASADR%  'Initialize  and declare CALL parameters
CLOSE #3
PRINT #l,  XON
FLAG% = 0
MD% = 0    'Mode 0 = initialization
CALL DAS8(MD%, VARPTR(BASADR%), FLAG%)
IF FLAG% o 0 THEN PRINT  "Installation Error"
CLS
'
 1502  GOSUB TEQUIL     Timing subroutines for temperature equilibration
GOSUB DROPDATA     Timing subroutine for allowing for data collection
OUT &H341,0   "Closes purge valve at end of run
END     'End of the program once all timing subroutines have been completed
'
TOTAL:
'  Subroutine for calculation of temperatures from thermistor voltage returns
MD% = 1:  LT%(0) = 7;  LT%(1) = 7
CALL DAS8(MD%, VARPTR(LT%(0)), FLAG%)
IF FLAG% <> 0 THEN PRINT "Error In Setting CJC Channel":  END
'  CJC stands for Cold Junction Channel which corrects for room temperature
MD%=4;  CJ% = 0
CALL DAS8(MD%, VARPTR(CJ%), FLAG%)
CJC = (CJ%)/10
2000  '  Get thermistor data
CH% = 0
COM(l) STOP:  status =1    '1 = stopped
'
GOSUB 2500
COM(l)ON:  status = 0
'  CH% specifies DAS*-PGA channel that EXP-GP is connected to (0-7).
'  D% (7)  is an integer data array to receive data for the thermistors from the channels.
DIM mvp(8)
FOR II = 0 TO 1   'Only two plates exist; hot and cold.
V = (D%(II) * 5!) / (2048!)    '! indicate whole numbers
mv = V *  1000    ' converts to millivolts
'
GOSUB 3300    'Perform linearization by piece-wise linear segmentation
mvp(II) = mv
'
NEXT II
COM(l) STOP:  status = 1
VIEW PRINT 1 TO 8
LOCATE 1, 1
FOR II = 0 TO 1
PRINT USING "Channel ## temperature = #####.#  deg. C. ";  II;  T(II)
NEXT II
COM(l) ON:  status = 0
```

```
'Heater controls for hot and cold plates.
b = (ct - 0.1):  c = (ct + 0.1)    'Cold plate temperature ranges
D = (ht - 0.1):  e = (ht + 0.1)    'Hot plate temperature ranges
IF c < T(0) AND e < T(l)  THEN TR = &H0   'Turns off both heaters
IF c < T(0) AND T(l) < D THEN TR = &H40   'Turns on only the hot plate heater
IF T(0) < b AND e < T(l) THEN TR = &H80   'Turns on only the cold plate heater
IF T(0) <b AND T(l) < D THEN TR = &HC0   Turns on both heaters
'
OUT &H340, TR
RETURN    'Returns to timing control loops in subroutines
'
2400  GOTO 2000    'Repeats scan of channels
'
2500 'Subroutine to convert EXP-GP channels to number of bits
LT%(0) = CH%;  LT%(1) = CH%:  MD% = 1
CALL DAS8(MD%, VARPTR(LT%(0)), FLAG%)
IF FLAG% <> 0 THEN PRINT "Error In Setting Channel":  END
'  Next select each EXP-GP channel in turn and convert it.
'  Digital outputs OOP1-4 drive the EXP-GP sub-multiplexer address, so use mode 14 to
'  set up the sub-multiplexer channel.
FOR MUX% = 0 TO 7
MD% = 14
CALL DAS8(MD%, VARPTR(MUX%), FLAG%)
IF FLAG% <> 0 THEN PRINT "Error in EXP-GP Channel Number":  END
'  Perform A/D conversion using mode 4 and transfer data to an array element.
MD% = 4
CALL DAS8(MD%, VARPTR(D%(MUX%)), FLAG%)
IF FLAG% <>0 THEN PRINT "Error in Performing A/D Conversion."
NEXT MUX%
RETURN
'
3000  VIEW PRINT 1 TO 25
CLS
RETURN
'
3300  'Interpolation routine to find thermistor temperatures.
' mv = thermistor voltage in millivolts
IF II = 0 THEN T(II) = 1 / (36.82865 - 8.803335 * LOG(mv) + 0.5265169 *
          (LOG(mv))^2):  RETURN:   'Cold plate thermistor calibration curve
IF II = 1 THEN T(II) = 1 / (31.09914 - 7.435571 * LOG(mv) + 0.4448631 *
          (LOG(mv))^2):  RETURN    'Hot plate thermistor calibration curve
RETURN
'
4900
MD% = 19    'Set DAS8-PGA
D%(0) = 9    'Range number 0, 8-15
CALL DAS8(MD%, VARPTR(D%(0)), FLAG%)
IF FLAG% <> 0 THEN PRINT "Error in Setting PGA":  END
RETURN
'
TEQUIL:
'This subroutine allows the cloud chamber plates time to reach their set temperatures
OUT &H341, &H1    'Makes sure that the valve is open to purge during this time
```

```
LOCATE 2, 45:  PRINT "Background Air"
TSTART = TIMER
TRUN = TIMER
WHILE TRUN < TSTART + 900    'Allows 15 minutes for temperature equilibration
GOSUB TOTAL
TRUN = TIMER
WEND
RETURN
'
DROPDATA:
'  This subroutine allows a set amount of time for drop data collection (purge valve is shut)
LOCATE 2, 45:  PRINT"
LOCATE 2, 45:  PRINT "Drop Data"
OUT&H341, 0   'Closes purge valve
TSTART = TIMER
TRUN = TIMER
WHILE TRUN < TSTART +  1200   'Allows for 20 minutes of drop data collection
GOSUB TOTAL
TRUN = TIMER
WEND
RETURN
```